REVIEW ARTICLE | AUGUST 09 2023

Transient flow modeling in viscoelastic pipes: A comprehensive review of literature and analysis

Vincent Tjuatja ; Alireza Keramat ; Bin Pan (彬 潘) ; Huan-Feng Duan (焕丰 段) ;
Bruno Brunone ; Silvia Meniconi

Physics of Fluids 35, 081302 (2023)
https://doi.org/10.1063/5.0155708

Physics of Fluids REVIEW pubs.aip.org/aip/pof

Transient flow modeling in viscoelastic pipes: A comprehensive review of literature and analysis

Cite as: Phys. Fluids **35**, 081302 (2023); doi: 10.1063/5.0155708
Submitted: 23 April 2023 · Accepted: 12 July 2023 ·
Published Online: 9 August 2023

View Online Export Citation CrossMark

Vincent Tjuatja,[1,a] Alireza Keramat,[1,b] Bin Pan (彬 潘),[1,b] Huan-Feng Duan (焕丰 段),[1,c] Bruno Brunone,[2,d] and Silvia Meniconi[2,e]

AFFILIATIONS

[1]Department of Civil and Environmental Engineering, The Hong Kong Polytechnic University, Hong Kong, China
[2]Department of Civil and Environmental Engineering, The University of Perugia, Via G. Duranti 93, Perugia 06125, Italy

[a]Electronic address: vincent.tjuatja@connect.polyu.hk
[b]Authors to whom correspondence should be addressed: alireza.keramat@polyu.edu.hk and bin89.pan@polyu.edu.hk
[c]Electronic address: hf.duan@polyu.edu.hk
[d]Electronic address: bruno.brunone@unipg.it
[e]Electronic address: silvia.meniconi@unipg.it

ABSTRACT

Water hammer or flow transients occur due to a sudden variation (over time) in flow properties that can lead to pipe system failure or damage. In addition, research on wave propagation and signal processing theories has developed different ways to detect anomalies in pipe systems. The two developments concerning pipe system safety and damage localization are of essential need in viscoelastic (VE) pipes, as their application in various industries is growing, given their favorable mechanical properties. With no literature review focusing on the topic, this paper aims to fill the current literary gap on transient waves in VE pipes. It highlights developments in the research field and elaborates on relevant water hammer concepts in VE pipes, including mathematical modeling, experimental setups, numerical solutions, parameter calibration, defect detection, and surge control. The comprehensive review concludes that a reliable transient wave model in viscoelastic pipes is yet to be fully confirmed despite the significant progress in the recent two decades.

I. INTRODUCTION

While the study of classical water hammer began in the mid or late nineteenth century, the research on water hammer in viscoelastic (VE) pipes has just started gaining popularity since the early 2000s with the increasing use of viscoelastic pipes such as polyvinyl chloride (PVC), high-density polyethylene (HDPE), polyethylene (PE), and other viscoelastic pipes. Despite its relatively young age, there have been many advancements in this research field over the past decades, as displayed in Fig. 1. With the topic being an increasingly popular research area, a literature review shall be prepared to highlight and explain the great discoveries in the field of water hammer in viscoelastic pipes.

In this paper, the developments and recent findings of water hammer in viscoelastic pipes are described, along with the relevant concepts such as its mathematical representation, experimental studies, numerical solution, calibration of viscoelastic parameters, time-domain, frequency-domain analysis, defect detection, and surge control based on viscoelastic properties. Vital publications on the topic, listed in Table I, are elaborated later in this paper. This review paper considers only research on water hammer in pipes made of viscoelastic materials. Transient behavior in the non-Newtonian fluid is not discussed in this paper.

In the analysis process, some typical assumptions are as follows. The fluid is assumed to have a constant density with space. The system is an isothermal system with no heat transfer during transient. Surface tension is presumed to be neglectable relative to the transient pressure.[1] Water flow is considered uniaxial and axisymmetric during the transient occurrence.[2] During turbulence, the eddy viscosity term for steady-state pipe flow remains applicable for water hammer flow. These assumptions are justifiable as the Mach number in a transient occurrence is significantly less than 1 (low Mach number approximation).[1,2] The viscoelastic effect in the pipe wall is assumed to be linear,[189] and the total strain in the pipe wall is representable by the superposition of static and dynamic strain.[3]

II. METHODOLOGY

In performing the literature review, four key steps are observed: the planning stage, the paper sourcing and screening stage, the knowledge enhancement stage, and the review stage. In the planning stage,

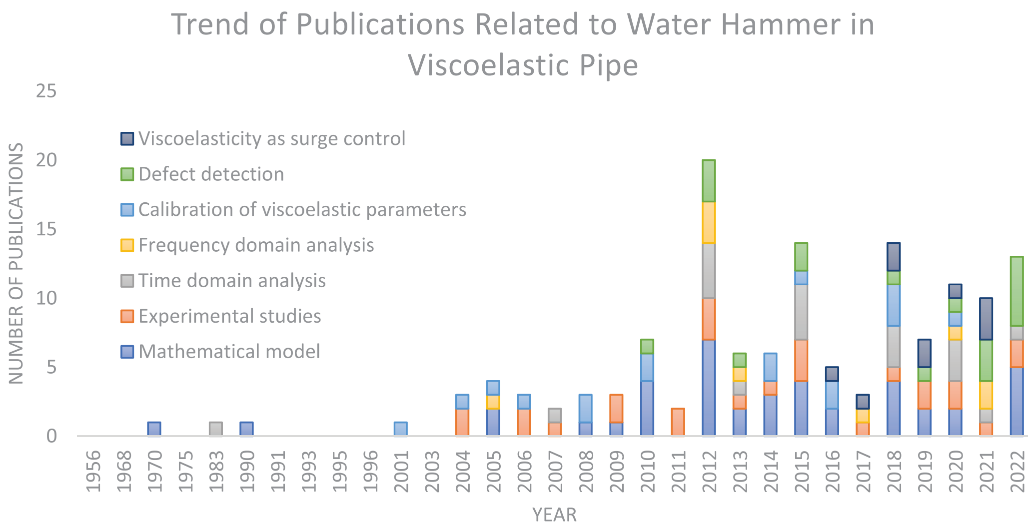

FIG. 1. The trend of research papers on water hammer in viscoelastic (VE) pipes over the past decades.

the scope of the study and preliminary paper structure is initially decided. Then, 250 research papers are sourced from the PolyU library database and Google Scholar. The collected research papers are not limited to the recent publication years to ensure a holistic review of the overall research development. Afterward, the papers are categorized and screened according to their relevance to the corresponding segment in the initial paper structure. The screening process is performed in a multi-staged manner with the sequence of title screening, abstract and introduction screening, and whole paper screening.

The gathered research papers are then read to enhance the authors' knowledge, specifically on modeling water hammer in viscoelastic pipes, e.g., using the method of characteristics (MOC) in the time domain and its closed-form numerical solutions. In this stage, several papers with significant contributions are identified. Considering the importance, these papers are then read multiple times to ensure an accurate understanding of the concept. Despite passing the screening stage, some papers are later found irrelevant to the topic and must subsequently be removed. The review stage is then started by explaining the general concepts related to the topic, followed by highlighting and comparing the critical contributions of various papers. The main challenges in reviewing the papers are figuring out the relevance and synthesizing some contrasting concepts. There are also papers in the literature, which have multiple contributions in various aspects. To accurately identify the linkage and contributions of the papers, the authors are required to read the paper in more detail. An overview of the methodology is shown in Fig. 2.

III. MATHEMATICAL MODEL

In modeling water hammer in viscoelastic pipes, the most important aspect is to integrate pipe-wall viscoelasticity into the classical water hammer equations. One method to model viscoelasticity is by introducing an additional viscoelastic term in the continuity equation based on the material behavior. When viscoelastic material is stressed,

TABLE I. Top ten most cited articles of water hammer in viscoelastic pipes based on Scopus accessed on June 3, 2022.

Article title	Authors
The dynamic effect of pipe-wall viscoelasticity in hydraulic transients: Part II—Model development, calibration, and verification	Covas *et al.*[9]
The dynamic effect of pipe-wall viscoelasticity in hydraulic transients: Part I—Experimental analysis and creep characterization	Covas *et al.*[103]
Fluid structure interaction with pipe-wall viscoelasticity during water hammer	Keramat *et al.*[4]
Parameters affecting water hammer wave attenuation, shape, and timing: Part I—Mathematical Tools	Bergant *et al.*[70]
Analysis of PVC pipe-wall viscoelasticity during water hammer	Soares *et al.*[150]
Water hammer pressure waves interaction at cross-sectional changes in series in viscoelastic pipes	Meniconi *et al.*[120]
Parameters affecting water hammer wave attenuation, shape, and timing: Part II—Case studies	Bergant *et al.*
System response function-based leak detection in viscoelastic pipelines	Duan *et al.*[16]
An investigation of pressure transients in viscoelastic pipes	Gally *et al.*
Water hammer control in pressurized-pipe flow using an in-line polymeric short section	Triki[178]

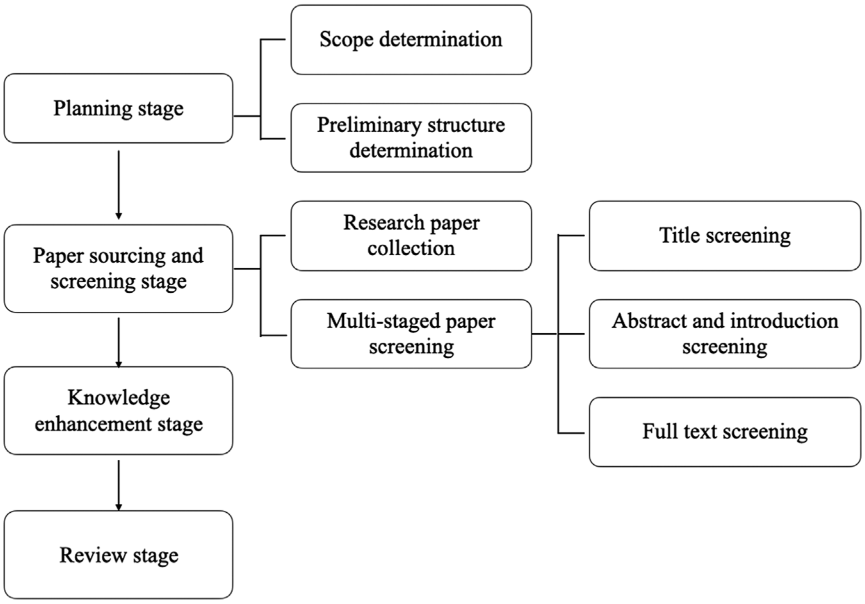

FIG. 2. The overview of literature review methodology.

it experiences both elastic and viscoelastic responses. The total strain experienced by the viscoelastic system can then be represented by a superposition of both elastic and viscoelastic strains, refer to Fig. 3. Viscoelastic representation based on material rheological behavior is achieved with the use of mechanical models. One prominent mechanical model is the Kelvin–Voigt (KV) model, as displayed in Fig. 4. In the figure, J_n represents the creep compliance of the n-th element spring, while η_n represents the viscosity of the n-th element dashpot. The KV model is elaborated in more detail in Sec. III B 1. When the viscoelasticity effect is neglected, a significant discrepancy in the modeling result is encountered, as seen in Fig. 5.

Another method is by adopting a frequency-dependent wave speed in the transient model because a significant manifestation of viscoelasticity on the wave propagation attributes to the wave speed. When a wave propagates in a viscoelastic material, wave speed changes with time or frequency. Consequently, wave speed can be represented as a time-dependent function that implicitly accounts for the creep behavior, unlike elastic consideration of the material's modulus of elasticity. Given this brief introduction, methods to take this time dependency of the water hammer response into consideration are elaborated in Sec. III A.

A. Classification based on the spatial coordinate system

Considering the spatial coordinate system, water hammer flows can be modeled in 1D, 2D, or 3D coordinate systems. A specific mathematical presentation is considered for the fluid flow for each coordinate system. In the 1D model, fluid flow is considered only in the axial direction. Due to this simplification, only laminar flow can be accurately represented, although promising approximations for turbulent flow have also been developed in the 1D model context. In 2D and 3D models, the 1D model can be extended to include fluid flow in the radial and azimuthal directions, respectively. With this arrangement, the prediction of the flow and pressure profile in 2D and 3D is more robust, allowing for the modeling of not only laminar flow but also turbulent flow effects with greater accuracy.

For the classical water hammer case, the governing equations were derived by Joukowsky,[5] Chaudhry,[6] and many other researchers. An extended work on the classical water hammer was also proposed by Skalak to account for additional damping and dispersion of the water hammer, which then became a pioneering study on fluid–structure interaction (FSI),[7] as elaborated later in Sec. III F.

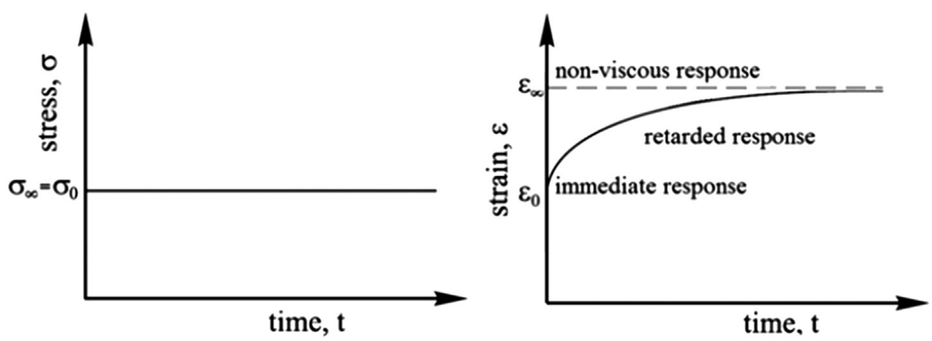

FIG. 3. Viscoelastic system response during creep test.[4]

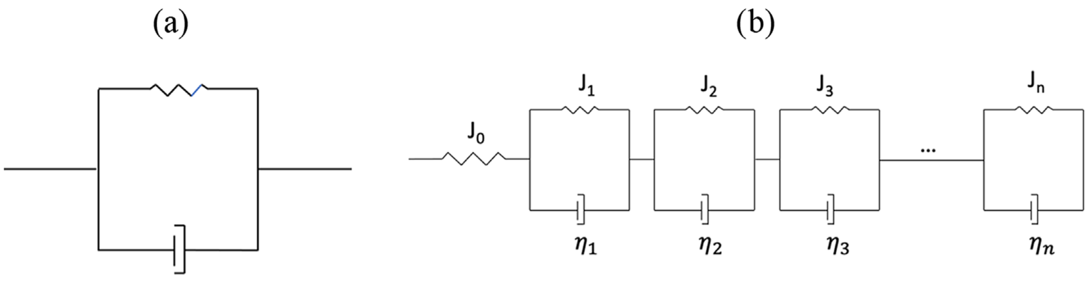

FIG. 4. Configuration of (a) one K–V element and (b) generalized K–V model.

Ghidaoui summarized the previously proposed sets of equations with Eqs. (1) and (2) for 1D, (3)–(5) for 2D, and (6)–(9) for 3D water hammer flow,[1]

$$\frac{1}{a^2}\frac{\partial H}{\partial t}+\frac{\partial U}{\partial x}=0, \tag{1}$$

$$\frac{\partial U}{\partial t}+\frac{\partial H}{\partial x}+\frac{\tau\pi D}{\rho A}=0, \tag{2}$$

$$\frac{1}{a^2}\left(\frac{\partial p}{\partial t}+u\frac{\partial p}{\partial x}+v\frac{\partial p}{\partial r}\right)+\frac{\partial u}{\partial x}+\frac{1}{r}\frac{\partial (rv)}{\partial r}=0, \tag{3}$$

$$\frac{\partial u}{\partial t}+u\frac{\partial u}{\partial x}+v\frac{\partial u}{\partial r}=-\frac{1}{\rho_0}\frac{\partial p}{\partial x}+\frac{\kappa+\frac{\mu}{3}}{\rho_0}\frac{\partial}{\partial x}\left(\frac{\partial u}{\partial x}+\frac{1}{r}\frac{\partial (rv)}{\partial r}\right)+v\left(\frac{\partial^2 u}{\partial x^2}+\frac{1}{r}\frac{\partial}{\partial r}\left(r\frac{\partial u}{\partial r}\right)\right)+f_x, \tag{4}$$

$$\frac{\partial}{\partial r}(p+\gamma z)=0 \quad \text{or} \quad \frac{p}{\gamma}+z=H(x,t), \tag{5}$$

$$\frac{\partial \rho}{\partial t}+\frac{\partial (\rho u)}{\partial x}+\frac{1}{r}\frac{\partial (r\rho v)}{\partial r}+\frac{1}{r}\frac{\partial (\rho w)}{\partial \theta}=0, \tag{6}$$

$$\frac{\partial (\rho u)}{\partial t}+\frac{\partial (\rho u^2)}{\partial x}+\frac{1}{r}\frac{\partial (r\rho uv)}{\partial r}+\frac{1}{r}\frac{\partial (r\rho uw)}{\partial \theta}=-\frac{\partial p}{\partial t}-\left(\kappa+\frac{\mu}{3}\right)\frac{\partial}{\partial x}\left(\frac{1}{\rho}\frac{D\rho}{Dt}\right)+\mu\nabla^2 u+\rho f_x, \tag{7}$$

$$\frac{\partial (\rho v)}{\partial t}+\frac{\partial (\rho uv)}{\partial x}+\frac{1}{r}\frac{\partial (r\rho v^2)}{\partial r}+\frac{1}{r}\frac{\partial (\rho vw)}{\partial \theta}-\frac{\rho w^2}{r}=-\frac{\partial p}{\partial r}-\left(\kappa+\frac{\mu}{3}\right)\frac{\partial}{\partial r}\left(\frac{1}{\rho}\frac{D\rho}{Dt}\right)+\mu\left(\nabla^2 v-\frac{v}{r^2}-\frac{2}{r^2}\frac{\partial w}{\partial \theta}\right)+\rho f_r, \tag{8}$$

$$\frac{\partial (\rho w)}{\partial t}+\frac{\partial (\rho uw)}{\partial x}+\frac{1}{r}\frac{\partial (r\rho vw)}{\partial r}+\frac{1}{r}\frac{\partial (\rho w^2)}{\partial \theta}+\frac{\rho vw}{r}=-\frac{\partial p}{r\partial \theta}-\left(\kappa+\frac{\mu}{3}\right)\frac{\partial}{r\partial \theta}\left(\frac{1}{\rho}\frac{D\rho}{Dt}\right)+\mu\left(\nabla^2 w-\frac{w}{r^2}+\frac{2}{r^2}\frac{\partial v}{\partial \theta}\right)+\rho f_\theta, \tag{9}$$

where x, r, and θ as the distance along axial, radial, and azimuthal direction, respectively; μ and κ as the dynamic and bulk modulus; ρ as the fluid density; f as the body force along the concerning direction; p representing pressure; u, v, and w representing velocity along the axial, radial, and azimuthal directions, respectively; H as piezometric head; τ representing shear stress; D/Dt as the material derivative in cylindrical coordinate; and ∇^2 as the Laplace operator in the cylindrical coordinate. Under this framework, research studies on 1D, 2D, and 3D modeling of water hammer with a special focus on the viscoelastic pipes are presented in the following.

1. 1D

While there are numerous papers regarding the 1D modeling of water hammer, some models are formulated to investigate other water hammer-related phenomena, such as pipe leakage, blockage, or fluid–structure interaction. Only the papers with the main contribution on 1D water hammer modeling in viscoelastic pipes are elaborated in this segment.

The earliest research of the 1D water hammer viscoelastic model dated back to 1970. Kokoshvili derived a numerical model of a one-dimensional unsteady flow in a single horizontal pipeline.[8] The water hammer behavior in the viscoelastic pipes was described using the Boltzmann model as a linear combination of elastic and retarded strain whose solution using the Fourier transform was derived.

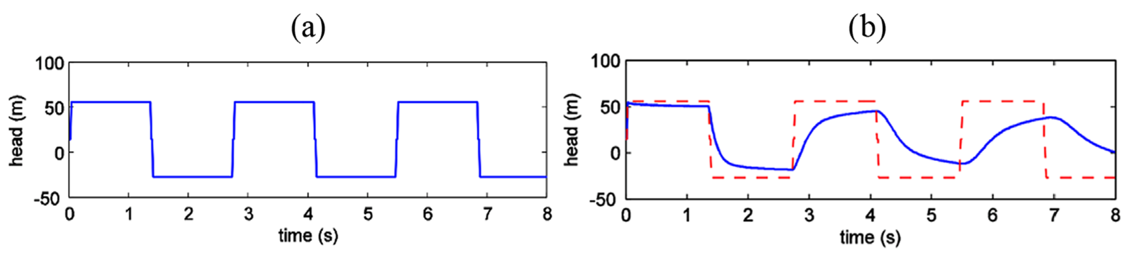

FIG. 5. Modeling result of (a) classical water hammer and (b) water hammer with viscoelasticity effect. The red dashed line in (b) represents the classical water hammer results.[3]

While the research on transients in viscoelastic pipes had become relatively stagnant over the extended period of approximately 30 years, the pioneering research that raised interest in the topic was conducted by Covas *et al.*[9] This study offered vast progress in the research of water hammer in viscoelastic pipes. However, new questions emerged in Covas *et al.*[9] work; for example, why various calibration parameters could be found for different steady-state flow rates. In parallel to this work, Pezzinga and Scandura[10] and Pezzinga *et al.*[11] found that viscoelasticity could result in far more damping in comparison with unsteady friction (UF), according to several experimental studies. More precisely, Brunone *et al.*[12] pointed out that it was impossible to simulate pressure damping in an HDPE without including a further term in the continuity equation. Even by considering an extremely large value of unsteady friction term in the momentum equation, the main features of transients in VE pipe could not be accurately captured. The mathematical contributions of these studies are discussed later in this section.

The viscoelastic impact in the continuity equation was represented by differential equations (10)–(12), according to Covas *et al.*,

$$\frac{\partial H}{\partial t}+\frac{a_0^2}{gA}\frac{\partial Q}{\partial x}+\frac{2{a_0}^2}{g}\frac{\partial \varepsilon_r}{\partial t}=0, \tag{10}$$

$$\varepsilon_r=\frac{\alpha D}{2e}\int_0^t\left[p(t-s)-p_0\right]\frac{\partial J(s)}{\partial s}ds, \tag{11}$$

$$J(t)=J_0+\sum_{k=1}^{N}J_k\left(1-e^{-\frac{t}{\tau_k}}\right), \tag{12}$$

with a_0 as the elastic wave celerity; g as gravitational acceleration; Q as the volumetric flow rate; ε_r as retarded strain; A as the cross-sectional area; α as the pipe wall coefficient; p as the pressure at a specific time; D and e as the pipe dimensions related to the diameter and wall thickness, respectively; J as the creep compliance with J_0 for the first spring and J_k for k-th number of KV elements; τ_k as the ratio between the dashpot's viscosity and spring's elastic modulus; and s as the integral's dummy variable.

Another method to model viscoelasticity was proposed by Landry *et al.*[13] using a system of a hydraulic resistor, an inductor, and a capacitor. With viscoelasticity, additional dissipation existed, leading to increased flow resistance. Thus, Landry *et al.* formulated hydraulic resistance as a function of volume viscosity term representing the equivalent viscoelastic damping of both fluid and wall

$$R_{ve}=\frac{\mu'}{A\rho g dx}, \tag{13}$$

with R_{ve} as the equivalent resistance in a viscoelastic system and μ' as the volume viscosity term related to the damping effect induced by viscoelasticity. The proposed model was found capable of accurately modeling the damping behavior in the system observed during the experiment. However, during the first oscillation, this model slightly overestimated the pressure head, which could then be corrected by an empirical correction factor.

Meniconi *et al.*,[14] Pezzinga *et al.*,[15] and Pezzinga *et al.*[11] adopted Covas *et al.*[9] 1D mathematical model concept but proposed a different numerical implementation for the rate of change of the retarded strain in the continuity equation. In their work, the retarded strain and its rate were consistent with the constitutive equation of each Kelvin–Voigt element, as follows:

$$\varepsilon_r=\sum_{k=1}^{n}\varepsilon_k, \tag{14a}$$

$$\frac{d\varepsilon_k}{dt}=\frac{1}{\tau_r}\left(\psi\frac{\rho gHD}{2eE_r}-\varepsilon_k\right), \tag{14b}$$

with ψ = dimensionless parameter based on pipe section dimension and constraint.

More specifically, Meniconi *et al.*[14] investigated their proposed VE formulations with an in-line valve as a boundary condition and assessed its impact on the water hammer pressures in VE pipes.

Several researchers corroborated the use of a single Kelvin–Voigt element that applied only one dashpot and spring arranged in parallel to make up for the time lag between the water hammer pressure and deformations in the pipe wall.[11,15,16] Intuitively, such a model introduced a new variable being the retarded strain ε_r to the continuity equation, for which a simple first-order ordinary differential equation, Eq. (14b), was adopted to close the formulation. The Italian group further demonstrated that a single KV element could provide theoretical results that were in good agreement with the experimental findings.[11,15] By using a single KV element, the continuity equation was no longer an integrodifferential equation, as seen in Eqs. (10) and (11). In other words, no summation was required over the solutions of several ordinary differential equations, as shown in Eq. (14a). Furthermore, contributions of Pezzinga *et al.*[11,15] to 2D modeling of water hammer waves are discussed later.

Another contribution to the modeling in the context of the generalized Kelvin–Voigt VE model aimed to include the impacts of deformations rather than the hoop or circumferential direction in the 1D model. Illustrated by Keramat *et al.*,[3,4,17] the retarded strain (ε_r) in Eq. (10) also had contributions from radial and axial deformations owing to the Poisson ratio of the pipe wall material. In these works, the three-directional stress–strain relations for the VE pipe were considered, while the axial deformation was ignored to eliminate the fluid–structure interaction. This correction in the hoop strain, which was neglected in previous works, eventually led to an improved presentation for the retarded strain term in Eq. (11) as follows:

$$\varepsilon_r=\frac{\alpha_{anch}D}{2e}\int_0^t\left[p(t-s)-p_0\right]\frac{\partial J(s)}{\partial s}ds, \\ \alpha_{anch}=(1-\upsilon^2)+\alpha_r\upsilon(1+\upsilon)\frac{2e}{D}, \tag{15}$$

α_{anch} = coefficient relating to the anchors' action, and α_r = averaging factor (1/2, or 3/4 according different reports; see Keramat and Haghighi for further details).[17] Eq. (15) offered a theoretical correction factor α_{anch} that accounted for the effects of deformations in other directions.

Another leap in modeling transients in VE pipes was accomplished by Ferrante and Capponi by incorporating a fractional derivative model for the stress–stress relation induced by waves.[18] Their model adopted

$$p(t)=\frac{2e}{D}k_\theta\frac{d^\theta\varepsilon_r}{dt^\theta}, \tag{16}$$

where $0\le\theta\le1$ ret. represents as the derivative order and k_θ represents as the creep parameter. The mechanical description of such a model may be called a "springpot," also referred to as fractional element, implying that a spring and dashpot are somehow mixed together.

For an accurate 1D model that is more consistent with the physical water hammer behavior, Keramat *et al.*[19] considered the time dependency of the Poisson ratio. The variation of Poisson's ratio with time was a known property of the VE materials that previous works neglected in their formulations. To this end, Keramat *et al.*'s model derived a more complete (but sophisticated) description of the hoop strain, leading the continuity equation to the following integrodifferential equation:

$$\frac{1}{A}\frac{\partial Q}{\partial z}+\frac{g}{{a_0}^2}\frac{\partial H}{\partial t}=-\frac{3}{4}\frac{\rho g D}{e}\frac{\partial I^c_{\tilde{H}}}{\partial t}+\frac{1}{36\kappa_p^2}\frac{\rho g D}{e}\frac{\partial I^r_{\tilde{H}}}{\partial t}, \tag{17a}$$

$$\begin{aligned} I^c_{\tilde{H}} &:= \int_0^t \tilde{H}(t-s)\frac{dJ}{ds}(s)ds \\ &= \sum_{k=1}^{N_{KV}}\left(\frac{J_k}{\tau_k}\int_0^t \tilde{H}(t-s)\mathrm{e}^{-\left(\frac{s}{\tau_k}\right)}ds\right) := \sum_{k=1}^{N_{KV}} I^c_{\tilde{H}k}, \end{aligned} \tag{17b}$$

$$\begin{aligned} I^r_{\tilde{H}} &:= \int_0^t \tilde{H}(t-s)\frac{dG}{ds}(s)ds \\ &= \sum_{k=1}^{N_{KV}}\left(-\frac{G_k}{\hat{\tau}_k}\int_0^t \tilde{H}(t-s)\mathrm{e}^{-\left(\frac{s}{\hat{\tau}_k}\right)}ds\right) := \sum_{k=1}^{N_{KV}} I^r_{\tilde{H}k}, \end{aligned} \tag{17c}$$

where G is the relaxation function whose parameters G_k and $\hat{\tau}_k$ are obtained using the creep coefficients through solving a nonlinear system of equations.

2. 2D

The 2D models are characterized by the flow types as either turbulent or laminar models. The quasi-2D modeling of transients in viscoelastic pipes is motivated by quasi-2D models in elastic pipes that are tested by ultrasonic Doppler velocimeter to predict velocity profiles, as implemented by Brunone and Berni.[20] While 2D models are mostly dominated by techniques for turbulent flow simulation, Wahba's[21] model is an exception. He developed a 2D numerical model to simulate the laminar transient behavior in viscoelastic pipes. Viscoelasticity was represented similarly to Meniconi *et al.*[14] proposition for the change of retarded strain with time. The derived set of governing equations was represented with Eq. (10) for the continuity and Eq. (18) for the momentum equation

$$\frac{\partial u}{\partial t}+u\frac{\partial u}{\partial x}=-g\frac{\partial H}{\partial x}+\frac{1}{\rho r}\frac{\partial(r\tau_{rx})}{\partial r} \quad \text{with } \tau_{rx}=\rho\nu\frac{du}{dr}. \tag{18}$$

For turbulent modeling of 2D water hammer, one of the earliest models was suggested by Pezzinga.[22] The proposed model was a quasi-2D model with the governing equations as follows:

$$\frac{dH}{dt}+\frac{a_0^2}{gA}\frac{\partial Q}{\partial x}=0, \tag{19}$$

$$\frac{\partial U}{\partial t}+g\frac{\partial H}{\partial x}+\frac{2\pi}{\rho}\frac{\partial(r\tau)}{\partial A}=0. \tag{20}$$

Pezzinga *et al.*[15] modified the previously proposed quasi-2D model to include the effect of viscoelasticity. They also compared their proposed 2D model against experimental results in terms of pressure variations and velocity profiles and identified the significant discrepancies between elastic and viscoelastic pipes. Their updated continuity equation is shown in Eq. (21), with the rate of change of retarded strain defined similarly to Meniconi *et al.*,[14]

$$\frac{dp}{dt}+\frac{\rho {a_0}^2}{A}\frac{\partial Q}{\partial x}+2\rho {a_0}^2\frac{d\varepsilon_r}{dt}=0. \tag{21}$$

The momentum equation remained the same, refer to Eq. (20), with shear stress based on Newton's law coupled with the mixing length model, as seen in Eq. (22),

$$\tau=-\rho\nu\frac{\partial u}{\partial r}-\rho l^2\left|\frac{\partial u}{\partial r}\right|\frac{\partial u}{\partial r}$$

with

$$l=\psi y e^{-y/R} \quad \text{and} \quad \psi=0.374+0.0132\ln\left(1+\frac{83\,100}{R_0}\right). \tag{22}$$

Other than modeling contribution, several studies on 2D modeling are targeted to increase understanding of the transient phenomenon. The effect of unsteady flow and viscoelasticity is found to be generally comparable. However, as time progresses, the viscoelastic effect becomes more dominant, especially in the case of viscoelastic retardation time being less than wave travel time along the pipeline.[23] With turbulence modeling, different phases of water hammer and their predominant feature can also be observed. However, when it comes to the comparison of velocity profile between elastic and viscoelastic pipes, which is the key manifestation of 2D modeling, a flatter profile is observed in viscoelastic pipes for a specific time and flow rate.[15] At wave acceleration and deacceleration phase, the major phenomena are the creation of shear waves near the pipe wall boundary and propagation of a previously constructed shear wave, respectively.[24]

3. 3D

Unlike the 3D modeling of classical water hammer, the number of research papers on the 3D modeling of water hammer in viscoelastic pipes is still relatively limited. Louati and Ghidaoui studied the propagation of high-frequency waves (HFWs) in which radial and azimuth modes experience excitation.[25] In this study, HFW was assumed to be inviscid, slightly compressible fluid in a rigid, unbounded, circular conduit. The result showed that the injected waves with a cutoff frequency experience significant wave dispersion behavior with a varying group velocity over a wide range of speeds, resulting in a large reduction in amplitude. Louati and Ghidaoui also analyzed the different factors affecting the HFW propagation range.[26] From this research, HFW's propagation range decreased with the increase in mode number due to the longer traveled path during the high mode.

Lai *et al.*[27] generally studied the effect of leaks during a high-frequency wave using computational fluid dynamics (CFD). The authors modified a 2D flow and applied a 3D equivalent area to present a representative 3D leak model, which was then validated. This paper also presented a depiction of wave propagation during transients.

With 2D water hammer modeling in viscoelastic pipes being sufficiently representative even for turbulent water hammer flows, the formulation of a 3D mathematical model with viscoelasticity becomes less preferable due to its complexity. However, referring to the classical water hammer case, a 3D model is found to yield superior conformity with the physical transient phenomenon compared to a 2D model.[28] Additionally, Siba *et al.*[29] suggested that when strong swirling exists within the system, 2D axial and radial pressure analysis is insufficient, and the water hammer problem shall be analyzed as a 3D flow. While there are some papers on 3D modeling of CFD in pipes,[27,30,31] there is currently no paper on 3D CFD modeling specifically for viscoelastic pipes. This research gap shall be filled in the future, given the need for more accurate water hammer modeling in viscoelastic pipes.

B. Material models

Material models refer to formulations developed based on the rheological behavior of material stress and strains, represented through the different configurations of springs and dashpot. In modeling water hammer in viscoelastic pipes, one can identify three adoptable material models, namely, Kelvin–Voigt, Maxwell, and standard solid model.

1. Kelvin–Voigt model

Kelvin–Voigt (KV) model is the most adopted material model. The generalized KV model consists of a spring and a series of n-number of KV elements representing elastic and retarded responses, respectively. A KV element is formed by the parallel configuration of spring and dashpot. During water hammer flow in viscoelastic pipes, peak pressure drops with time due to damping behavior accounted by pipe material viscoelasticity. When the generalized Kelvin–Voigt model is applied with the correct approximation of KV elements, this model is capable of modeling pipe wall viscoelasticity with a high agreement with the experimental result, including the pressure damping phenomena. This material model is commonly adopted by many researchers such as Covas *et al.*,[9] Wahba,[21] Shamloo and Mousavifard,[24] Pezzinga *et al.*,[15] Duan *et al.*,[23] and many others. The arrangement of the Kelvin–Voigt element and general Kelvin–Voigt model can be seen in Figs. 6(a) and 6(b), respectively.

2. Maxwell rheological model

In the Maxwell model, springs and dashpots are connected in series. Generally, the Maxwell model is more commonly used to model viscoelastic fluid. However, Morvarid *et al.*[32] applied the Maxwell model to model the viscoelastic response in VE pipes. In this model, with constant applied strain, the stress decreases exponentially with time, displaying a similar behavior to stress relaxation in polymeric and viscoelastic pipes. While Morvarid *et al.*[32] study did not specifically compare the performance of the Maxwell model relative to the commonly adopted KV model, pressure fluctuation dampening was observed in the numerical result, similar to the KV model. The arrangement of the Maxwell model is shown in Fig. 6(c).

3. Standard solid model

The standard solid model is a recently proposed mechanical model specifically developed for high-density polyethylene (HDPE) pipes. In this model, two branches work in parallel, with one branch consisting of only one elastic element and the other branch with a combined configuration of elastic and damping elements arranged in series. Refer to Fig. 6(d) for the arrangement of the standard solid model. When subjected to stress, the elastic branch represents the instantaneous response, while the branch with elastic and damping elements represents the long-term response. While this model can represent long- and short-term responses along with the stress relaxation in material, this model is only applicable within the pipe wall's elastic deformation limit.[33]

4. Consideration of the time dependency of Poisson's ratio

In addition to the previously mentioned mathematical models, Keramat *et al.*[19] suggested a mathematical model, which considered the effect of time-varying Poisson's ratio for viscoelastic pipes. The

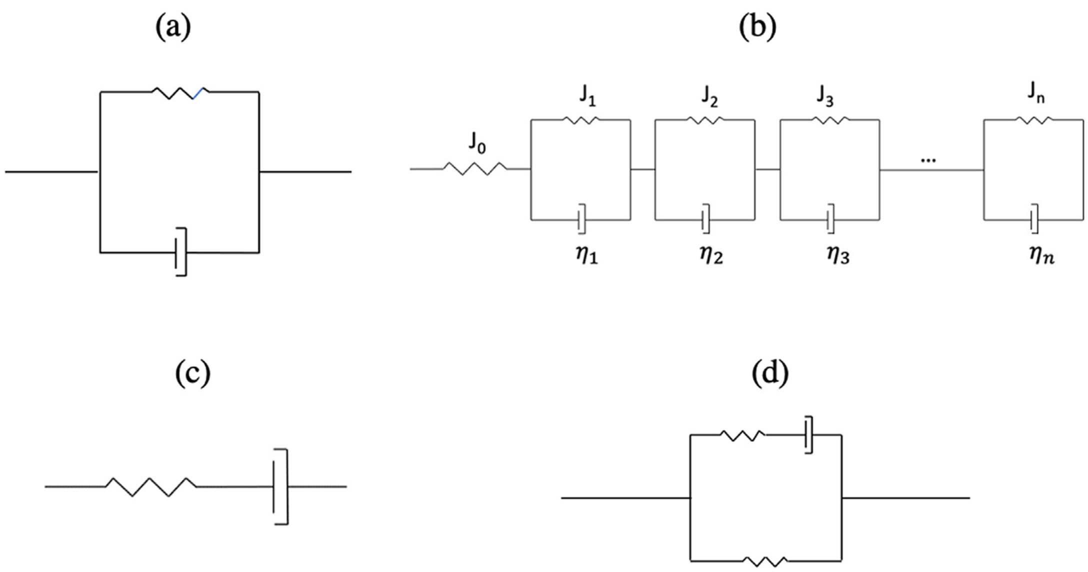

FIG. 6. Material model of (a) one Kelvin–Voigt element, (b) generalized Kelvin–Voigt model, (c) Maxwell model, and (d) standard solid model.

proposed model was expressed as the combination of the relaxation function and constant bulk modulus, with the relaxation function as a function of the specific creep function based on the viscoelasticity of the pipe material. By incorporating the time-dependent Poisson's ratio and unsteady friction models, a relatively more precise water hammer analysis was achieved without additional calibration. Likewise, the creep function obtained from measurements was closer to the experimental creep function when compared to the previous viscoelastic models.

C. Unsteady friction models

The velocity profile at each cross-section in the water hammer transforms over time. With the changing velocity profile, it is then expected that the induced friction is changing unsteadily over time, as the pipe–fluid friction is a function of the fluid's changing velocity profile. In the case of water hammer in viscoelastic pipes, the coupled effect of viscoelasticity (VE) and unsteady friction (UF) complicates the transient analysis. A comparison between classical water hammer, transients with unsteady friction, and water hammer in viscoelastic pipes with unsteady friction is shown in Fig. 7. Compared to the classical water hammer, the inclusion of unsteady friction dampens the pressure distribution, with additional consideration of pipe wall viscoelasticity further increasing the head dissipation during transients. The VE effect is typically modeled in the continuity equation, as shown in Sec. III A, while UF is integrated into the momentum equation. For an accurate representation of the water hammer dynamics, both UF and VE effects must be modeled in the system.[9]

Over the years, many researchers have proposed different approaches to unsteady friction. The most straightforward unsteady friction representation assumes that it only depends on the instantaneous mean flow velocity, as adopted by Hino *et al.*[34] and Brekke.[35] However, this method severely oversimplifies the complexity of unsteady friction and is often considered insufficient for modeling purposes.

Several researchers also suggested that unsteady friction depended on the instantaneous average velocity V and local acceleration dV/dt,[36–38] governed by the equation as follows:

$$f_u = f_s + k\frac{D}{V^2}\frac{dV}{dt}. \tag{23}$$

Brunone *et al.*[39–41] proposed another unsteady friction equation based on the fluid's average velocity V, local acceleration $\partial V/\partial t$, and convective acceleration $\partial V/\partial x$. Brunone's model was then modified by Vitkowsky to account for the changing velocity direction in the case of the water hammer phenomenon by introducing a new function sign $(V) = (+1 \text{ for } V \geq 0 \text{ or } -1 \text{ for } V < 0)$.[42] Brunone's model and Vitkowsky's formulation are shown in Eqs. (24) and (25), respectively,

$$f_u = f_{\text{quasi-steady}} + \frac{kD}{V|V|}\left(\frac{\partial V}{\partial t} - a_0\frac{\partial V}{\partial x}\right), \tag{24}$$

$$f_u = f_{\text{quasi-steady}} + \frac{\text{kD}}{V|V|}\left(\frac{\partial V}{\partial t} + a_0 \,\text{sign}(V)\frac{\partial V}{\partial x}\right). \tag{25}$$

Unsteady friction could also be derived according to the cross-sectional distribution of the flow velocity.[43–45] The model, also known as cylinder model, was formulated according to the mass and

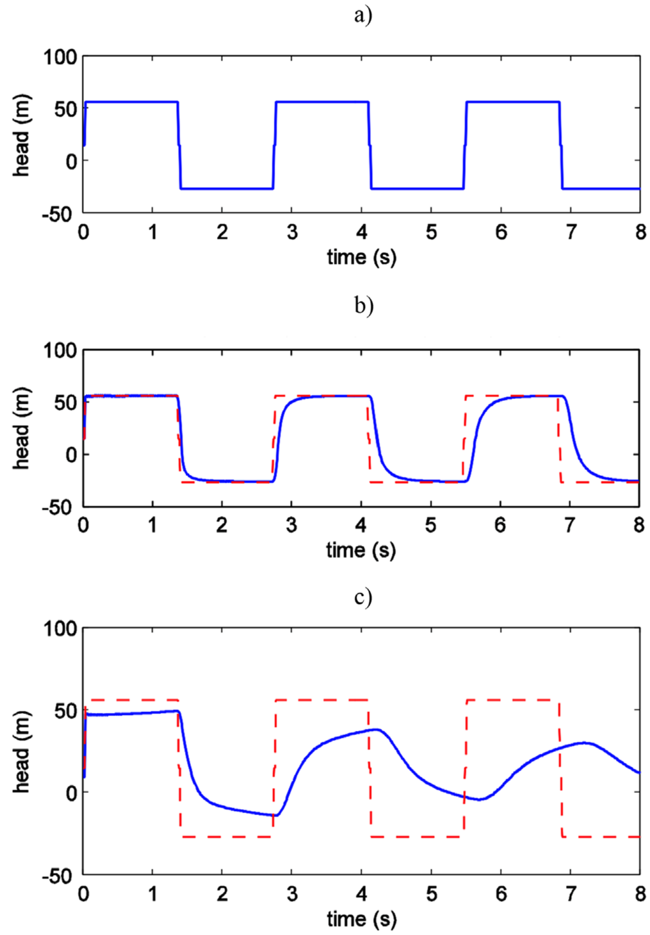

FIG. 7. Numerical modeling of (a) classical water hammer, (b) water hammer with unsteady friction effect, and (c) water hammer with unsteady friction and pipe wall viscoelasticity.[3]

momentum equilibrium as a function of mass flux in a specific pipe shell segment. The derived governing equations are as follows:

$$\frac{\text{g}}{{a_0}^2}\frac{\partial H}{\partial t} + \frac{\text{g}u_j}{{a_0}^2}\frac{\partial H}{\partial x} + \frac{\partial u_j}{\partial x} = \frac{1}{\rho A_j}\left(\dot{m}_{j-1} - \dot{m}_j\right), \tag{26}$$

$$g\frac{\partial H}{\partial x} + \frac{\partial u_j}{\partial t} + u_j\frac{\partial u_j}{\partial x} = \frac{1}{\rho A_j}\left\{\frac{1}{2}\dot{m}_{j-1}(u_{j-1} + u_j) - \frac{1}{2}\dot{m}_j(u_{j+1} + u_j) + F_{j-1} - F_j\right., \tag{27}$$

with a_0 as the wave speed, H as the local pressure head, u_j as the fluid velocity along the axial direction of cylinder j, A_j as the cross-sectional area of j-th cylinder, and $\dot{m}_j$ and F_j as the mass flux and local shear force per unit length of cylinder j, respectively.

Several researchers, such as Vennatrø[46] and Svingen,[47] presented another method for unsteady friction by using instantaneous average velocity V and diffusion term $\partial^2 V/\partial x^2$. However, generally, a more comprehensive approach to model unsteady friction is by considering the fluid velocity profile through the convolution term.

Zielke first proposed a convolution integral to model transient laminar pipe flow.[48] The model was represented as a function of dimensionless time τ, which depended on the time, kinematic viscosity, and pipe radius. The proposed convolution integral allocated more weight at a low dimensionless time of $\tau < 0.02$, which decreased with a higher dimensionless time:

$$\text{for } \tau \le 0.02, \quad W(\tau) = \sum_{i=1}^{6} m_i \tau^{(i-2)/2}, \tag{28}$$

$$\text{at } \tau > 0.02, \quad W(\tau) = \sum_{i=1}^{5} e^{-n_i \tau}. \tag{29}$$

Vardy *et al.*[49] then proposed a new model, shown in Eq. (30), by extending Zielke's model to account for turbulent flow at low Reynolds number through the laminar annulus core assumption,

$$W(\tau) = \frac{1}{4} f \mathrm{Re} \sum_{k=1,2,3,.}^{\infty} \exp\left(-\frac{(k\pi f \mathrm{Re})^2 \tau}{16}\right). \tag{30}$$

The model was then improved by Vardy and Brown.[50] Assuming viscosity variation to be linear within the thick shear layer with a uniform velocity core (frozen viscosity assumption), a new model, dependent on dimensionless time τ and viscosity ratio σ, was proposed to be applied even to high Reynolds number turbulent flow. The frozen viscosity assumption was validated by the authors by comparing the proposed viscosity distribution with the experimental evidence by Laufer. This assumption was found adequate to portray the turbulence occurrence within pipes, characterized by the linearly increasing viscosity from the pipe radius toward the center of the pipe and the constant viscosity within the central pipe region. The previous model by Vardy *et al.*[49] was found to be a case of $\sigma = 1$ for the proposed model:

$$W(\tau, \sigma) = \frac{A^* \exp(-B^* \tau)}{\sqrt{\tau}}, \quad \text{where } A^* = \frac{1}{2\sqrt{\pi}} \quad \text{and} \quad B^* = f(\sigma). \tag{31}$$

Vardy and Brown discovered that their previous model underestimated the amplitude of unsteady shear stress due to the uniform velocity core assumption.[51] An improved model was then proposed by assuming uniform core turbulent viscosity with radial viscosity distribution.

Urbanowicz *et al.*[52] combined Zielke's laminar and Vardy–Brown's turbulent model into a universal model, which included the effect of cavitation. The proposed universal model simulated transients with a wide range of Reynolds number. This method successfully removed numerical errors during flow type change from laminar to turbulent flow and vice versa.

While convolution integral may accurately represent unsteady friction, it is relatively cumbersome to implement with extensive time and computational requirements. Weighting function approximation is then developed to tackle this issue. Over the years, many researchers strived to propose an effective weighting function approximation. Trikha first proposed an approximation of Zielke's laminar model as a sum of three exponential terms.[53] While this method successfully modeled Zielke's model in most cases, several computational errors were found for a small dimensionless time. The limitation of Trikha's approximation was tackled by Kagawa *et al.*[54] by approximating Zielke's model with ten exponential terms. Vardy and Brown then developed a simple method based on the approach by Kagawa *et al.*, capable of approximating both Zielke's laminar model and Vardy Brown's turbulent model by discrete point "knots"-based approximations.[55]

Similar to Vardy and Brown,[55] Vitkovsky *et al.*[56] also improved Kagawa's approximation for both Zielke and Vardy–Brown model, but by optimizing Kagawa coefficient and implementing single diamond grid MOC, eliminating grid separation error. Zarzycki *et al.*[57] proposed another approximation similar to Trikha but with eight exponential terms. This method increased the computational efficiency for approximating Zielke's laminar model. However, this approximation was inaccurate for Vardy–Brown's turbulent model, especially at the increased Reynolds number. Urbanowicz presented an analytical solution for quick determination of two or three exponential term effective approximations.[58] While this method was relatively simpler to use, many constants, which described individual solutions, shall be introduced in the computer program, along with the correct choice of formula corresponding to the selected MOC grid.

D. Energy analysis

Energy analysis is a crucial part of understanding the physical behavior of a phenomenon, especially in water hammer, in which the system characteristics continuously change with time. More specifically, in viscoelastic pipes with significant energy dissipation, a better understanding of the water hammer phenomenon can be achieved by performing the energy analysis.

Karney derived an energy equation based on the momentum and continuity equation for general transient pipe flow.[59] The proposed energy equation was related to the change in total kinetic energy, change in total internal energy, rate of viscous dissipation, and rate of work done in the system. Duan *et al.*[60] further distinguished the work done in the system as the work done in the system through the pipe ends and on the pipe walls. When analyzed by the Fourier analysis, energy dissipation due to VE was found to be closely dependent on wave frequency and viscoelastic relaxation frequency. The ratio between the two could then be interpreted as the number of energy transfers between fluid and pipe wall, leading to significant VE damping with the increase in the corresponding ratio.

Wu *et al.*[61] performed an energy analysis on the quasi-2D friction model of viscoelastic pipes to determine the correlation between the Reynolds number and work done attributed to frictional and viscoelastic terms. From this study, the work done due to viscoelasticity and friction increased over time with a higher Reynolds number. Viscoelastic term produced sinusoidal energy fluctuation, which existed longer in the smaller initial Reynolds number before approaching constant value with time. Friction term induced high initial energy dissipation, which decreased over time until approaching a constant value. With a higher initial Reynolds number, the energy dissipation by the friction component increased while the opposite applied to the viscoelastic component.

To facilitate an energy analysis, an energy phase diagram comparing the potential and kinetic energy in the system during transient is formulated.[59] Lee proposed an energy phase diagram with dimensionless parameters corresponding to the ratio of potential energy and kinetic energy during and before transients.[62] The energy phase diagrams were investigated by Pan *et al.*[63] to identify energy variations

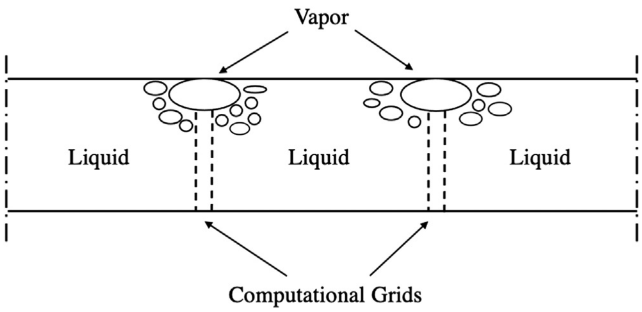

FIG. 8. A sketch of DVCM.

during transients in VE pipes. During small perturbations, steady friction was the most significant contributor to energy dissipation. However, the viscoelasticity effect became more crucial during higher excitation and valve oscillation frequency.

E. Cavitation and column separations

Cavitation, which in the case of water hammer in the 1D analysis is known as column separation, is an occurrence during which water pressure drops to the vapor pressure, forming vapor cavities in the system. As fluid flows in segregated directions, the vapor cavity grows. However, when fluid changes direction due to the transient waves and boundary effects, with both fluid segments compressing the vapor cavity, a significant amount of energy is suddenly released, causing major damage to the piping system. Due to its potential hazard, the cavitating behavior during fluid transient has been extensively studied by many researchers.

Over the years, many models have been proposed to represent cavitating behavior. The most frequently adopted method is the discrete vapor cavity model (DVCM), which was first developed by Thibessard[64] and improved by many researchers such as Streeter,[65] Tanihashi and Kasahara,[66] and Wylie and Streeter.[67,68] In this model, pipelines are divided into computational segments in which cavities are formed when the computational pressure drops below the vapor pressure, similar to cavitation's physical behavior. Among computational sections with cavitation, a constant pressure wave speed is assumed.[69] A schematic figure of DVCM is depicted in Fig. 8.

In the viscoelastic pipeline, DVCM was applied by Keramat and Tijselling,[3] Bergant *et al.*,[70] Keramat *et al.*,[71] and Soares *et al.*[72,73] Viscoelasticity was found to dampen the pressure induced by column separation as seen in Fig. 9.[3,71,74] When MOC was used, the literature recommended the use of the staggered grid as opposed to the rectangular grid.[75,76] However, Keramat *et al.*[71] proposed an improved rectangular MOC grid based on a weighted time integration, which enhanced the cavitation prediction of a rectangular grid in the viscoelastic pipeline. When DVCM was applied in viscoelastic pipes, errors indicated by unrealistic overpressure and energy dissipation existed during gas expansion and contraction.[72] Considering this error, Soares *et al.*[71,72] proposed using the discrete gas cavity model (DGCM) as a better option.

Originally presented by Brown[77] and developed by De Vries,[78] Provoost,[79] Provoost and Wylie,[80] and Wylie,[81] DGCM is a modification of DVCM that incorporates the ideal gas law. In this model, cavitating behavior is simulated with entrained air located equally distributed along the pipeline. The air pocket is analyzed based on the pressure–volume relation (ideal gas law), and the position is assumed to be constant with the variation of flow direction during the transient.

The ideal gas assumption in DGCM is more appropriate in modeling the gas cavity size transformation when compared to the simple vapor pressure assumption in DVCM.[72] However, during steepening pressure waves, shock waves may be formed, as shown in Fig. 10, which are not properly modeled in DGCM.[69] When shock wave modeling is necessary, interface models and bubble flow models shall be more suitable.

Bubble models, first introduced by Kranenburg,[82] are two flow models, which differentiate the pure liquid region and cavitation region with the liquid–vapor mixture. Initially, without transient, fluid consists of pure liquid. Under transient, with pressure drop below the vapor pressure, vapor exists within the liquid distributedly. The mixture of liquid and vapor is expressed in terms of liquid volume fraction and is assumed to satisfy the ideal gas law. In the literature for viscoelastic pipes, this model has been applied by Hadj-Taïeb and Hadj-Taïeb,[74] Urbanowicz and Firkowski,[83] and Urbanowicz *et al.*[84] with high conformity with experimental validation.

Other models for cavitating transient in viscoelastic pipes include the generalized interface vaporous cavitating model (GIVCM) and the discrete Adamkowski cavitating model (DACM). GIVCM, first proposed by Bergant and Simpson,[85] is an improved version of DVCM that combines one-phase and two-phase flow. When vapor cavities are formed and distributed, the system is analyzed as a one-phase flow. After the distributed vaporous cavitation region stops expanding, the system is analyzed as a two-phase flow with liquid and vaporous phases. The shock wave is modeled with shock equations in the continuity and momentum equation. Despite its complexity, GIVCM

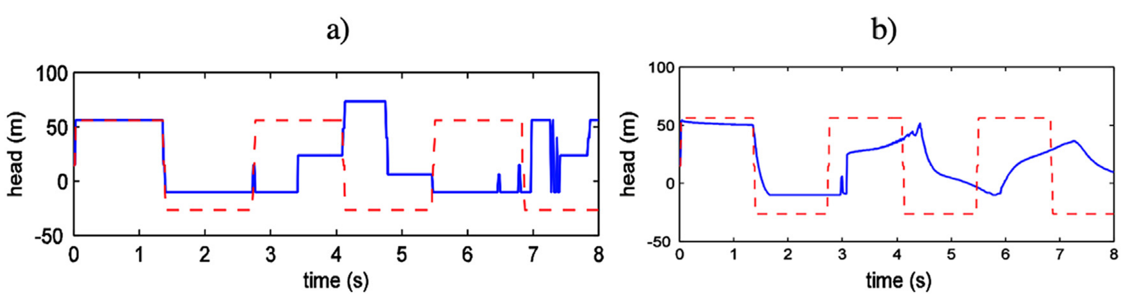

FIG. 9. DVCM modeling of cavitation for (a) classical water hammer and (b) water hammer in viscoelastic pipes.[3]

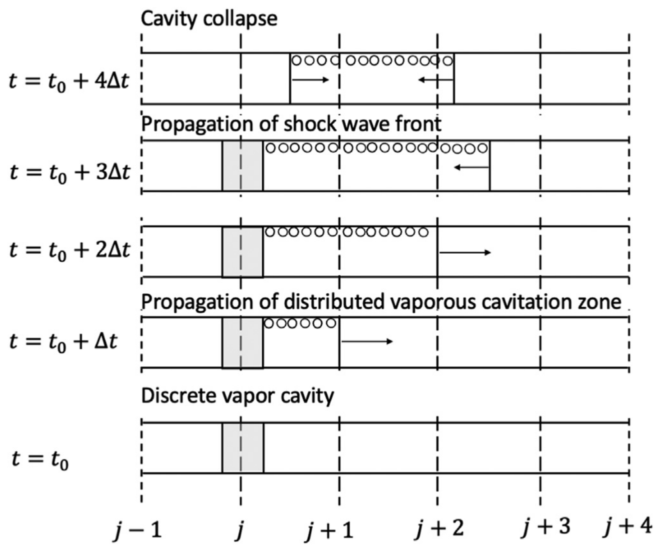

FIG. 10. Shock wave formation and propagation.

allows direct tracking of the actual column separation phenomenon, leading to a better understanding of transient behavior.[75] Additionally, GIVCM is found to have a better correlation with experimental data when compared to DVCM, especially regarding the timing and pressure magnitude.[86]

The discrete Adamkowski cavitating model (DACM) is another viable option for modeling cavitation. Similar to GIVCM, DACM is also an improved version of DVCM. In DACM, a vaporous zone is assumed to replace several vapor zones with equivalent mass and energy conservation law. The volume of the representative cavity is equal to the sum of all cavities' volumes along the pipeline. Two liquid flows separated by a cavity with two streams are substituted with one continuous fluid stream. Wall shear stress is modeled as a single-phase flow. DACM is found to yield a similar result to the experimental data with performance comparable to bubble models.[84]

F. Fluid–structure interaction (FSI)

Fluid–structure interaction is a research area regarding the relation between fluid flow and the surrounding boundary structure. While water hammer modeling may accurately predict the peak pressure and transient period, discrepancies in terms of wave damping, physical pressure fluctuations, and dispersion attributed to FSI are often observed when compared to the real-life system, addressed by Skalak's pioneering study on FSI.[87] Study in fluid–structure interaction is important, especially when there is a motion of the system. In this case, treating water and pipe separately based on the traditional analysis is inaccurate. Instead, an inter-related coupled system of water and pipe shall then be analyzed.[88]

In 1D modeling, the fluid–structure interaction consists of three coupling methods: junction, Poisson, and friction coupling. Junction coupling is a situational coupling within boundary condition changes such as pipeline bending, constriction, or branching. Poisson coupling exists everywhere along the pipe length and is related to how the axial strains in the pipe wall influence the fluid flow. The friction coupling, like the Poisson coupling, occurs throughout the pipe length and is attributed to the friction between the pipe wall and fluid, affecting the system's pressure fluctuations. The different coupling mechanism of FSI is displayed in Fig. 11.

Classically, the water hammer phenomenon is described with two equations. Another two equations are introduced to account for structural vibration behavior resulting from FSI, resulting in a four-equation model.[89–93] With more degrees of freedom, more equations are needed to model the FSI behavior accurately. Six-equation model[94] and eight-equation model[95] have also been proposed to model the radial inertial force in the pipe wall and planar pipe systems, respectively. However, the most complete inclusion of FSI shall be represented with fourteen partial differential equations (PDE) to describe the axial, lateral, and torsional motion.[91,96]

In viscoelastic pipes, FSI is crucial, especially in the early development of transients. Afterward, the viscoelastic effect becomes a more dominant effect, dampening FSI-induced oscillation, refer to Fig. 12.[3,32,97–99] With the dampening effect, displacements and stresses in the system are diminished significantly, leading to less pressure

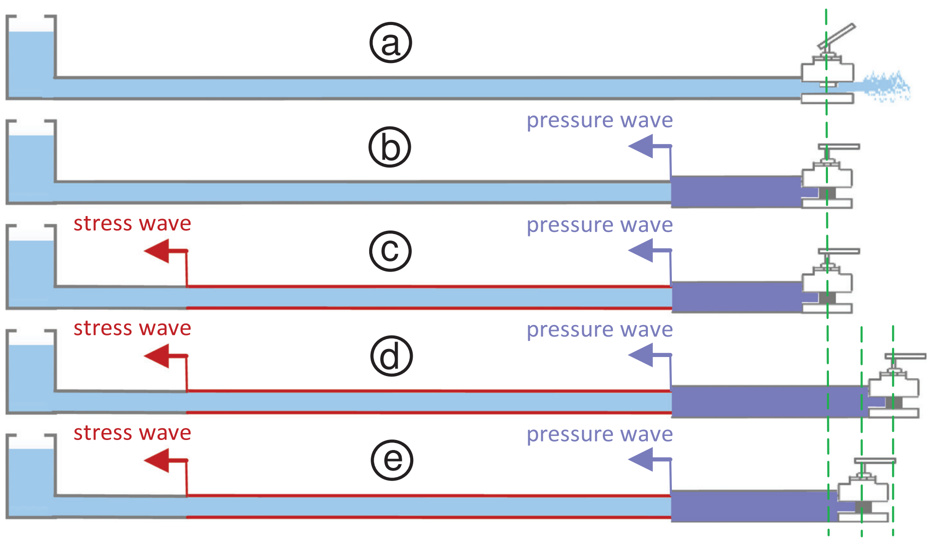

FIG. 11. Different mechanisms of FSI (a) without water hammer, (b) classical water hammer, (c) Poisson coupling, (d) junction coupling, and (e) Poisson and junction coupling.[4]

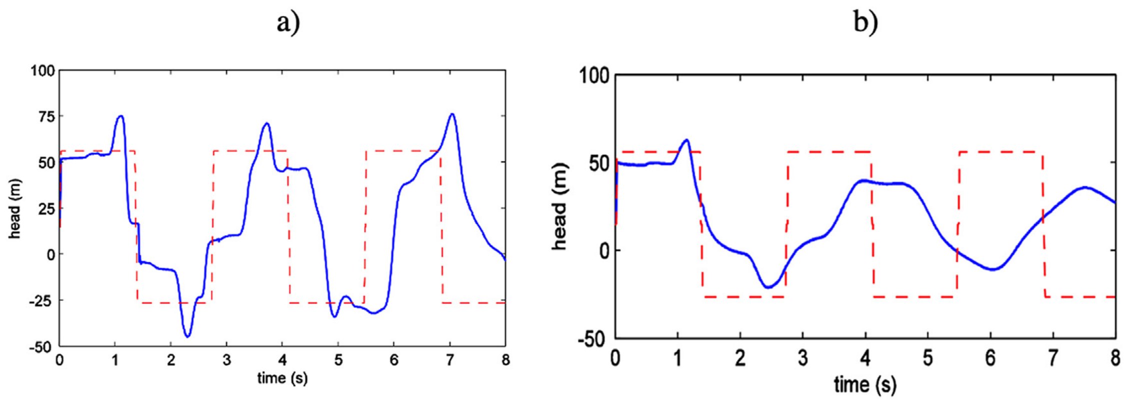

FIG. 12. FSI modeling considering Poisson, junction, and friction coupling in (a) classical water hammer and (b) water hammer in viscoelastic pipes.[3]

jump and elimination of high-frequency fluctuation.[100] When analyzed in the frequency domain, Poisson coupling causes a significant frequency shift from the natural frequencies. While junction coupling may be important depending on the system specification and boundary conditions, the effect may be neglected in the case of a restrained end section of pipe,[99] which is realized by a significant support stiffness thereof. Despite the validity of the potential simplifications, when accurate modeling of FSI behavior is required, all three coupling mechanisms should be accounted for.

Similar to the classical water hammer case, in viscoelastic pipes, numerical modeling of FSI may be based on four[97,98] or fourteen differential equations,[101] but with the inclusion of the pipeline's retarded behavior. Modeling based on a simplified viscoelastic model of two equations has also been executed and proven adequate, as performed by Guidara *et al.*[98] However, the proposed two-equation model was found incapable of modeling the junction coupling effect and stress wave velocity effect. Thus, the use of two equations simplified model was only applicable for instances with minimal change of boundary condition in a relatively long viscoelastic pipe with multiple axial stops, where the effect of stress wave velocity on the pressure variation was thereby negligible.

As FSI is closely related to the motion of the system, research on the different support mechanisms, namely, axial, shear, or sliding-shear mechanisms in FSI in the viscoelastic pipeline, has also been performed. Comparison between axial and shear mechanisms shows that supports with shear modeling have a better performance with higher practicality when compared to axial modeling. Regarding the sliding-shear mechanism, the performance depends heavily on the magnitude of frictional force. In high frictional force, no sliding occurs, and the system behaves similar to the shear mechanism. Conversely, for low frictional force, FSI overcomes frictional force, leading to sliding behavior. In this condition, the dissipation by FSI is increased due to the mobilization of the system. Considering its robustness, the use of a sliding-shear mechanism is more advisable.[102]

IV. EXPERIMENTAL STUDIES

Through experimental studies, researchers are able to investigate the different components of the water hammer phenomenon, such as pressure variation and wave reflection, validate numerical models or perform experimental calibration of creep functions as the representing viscoelastic parameter for the specific piping system. Experimental apparatus shall typically consist of a piping system of interest, a downstream valve to simulate the water hammer phenomenon, the data collection tools such as pressure transducers, flow meters, or strain gauges (for FSI experiments to analyze the pipe system's movement) with an appropriate choice of sampling frequency conforming to the Nyquist–Shannon sampling theory, data recording tools consisting of data logger or computer to record and monitor the collected data, and other experiment control measures depending on the experimental circumstances and purposes (laboratory test or field test).

A. Laboratory test

1. Single pipe

Over the years, many laboratory experiments have been conducted on a single viscoelastic pipe. Considering its abundance and the scope of this paper, only several prominent laboratory experiments on a single pipe are further elaborated, namely, the experiment in the Imperial College, the Instituto Superior Técnico, the Hong Kong University of Science and Technology, and the University of Perugia.

a. Imperial College (London, UK). Covas *et al.*[103] analyzed the dynamic effect of transients in high-density polyethylene (HDPE) pipe during different flow conditions. Overall pressure damping was observed in consecutive pressure waves, attributed to the predominant viscoelastic behavior. Calibration of viscoelasticity was also performed by creep test, and high compliance was then found between the experimentally obtained creep function and pipe rig pressure and strain measurement. However, the experimental setup was unable to obtain the creep function for a very short time and the elastic creep function. The Imperial College experiment is depicted in Fig. 13.

b. Instituto Superior Técnico (Lisbon, Portugal). Similar to Covas *et al.*,[103] Ramos and Covas also observed the dynamic response during transient behavior in HDPE pipes by conducting two experiments, as seen in Fig. 14, and found the significant contribution of pipe material viscoelasticity on pressure wave damping.[104] However, an additional contribution of the paper was the effect of pipe leakages in a pipeline.

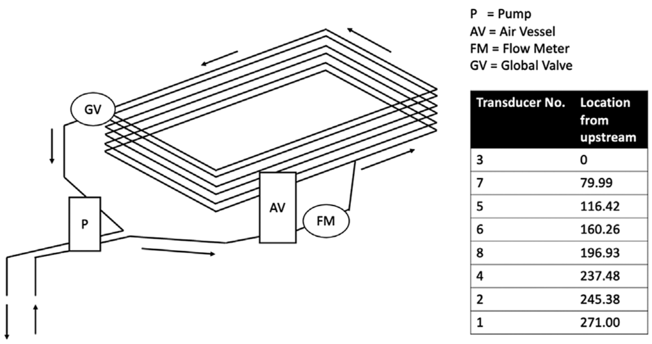

Transducer No.	Location from upstream
3	0
7	79.99
5	116.42
6	160.26
8	196.93
4	237.48
2	245.38
1	271.00

FIG. 13. Experimental apparatus at the Imperial College.

Leakage induced a sudden drop in the first pressure wave and behaved as a relief valve, increasing wave dissipation during the transient. It was also found that by analyzing the first reflected wave, the leak location and size could be estimated.

c. Hong Kong University of Science and Technology. Another experiment with a contribution to leakage in viscoelastic pipes, shown in Fig. 15, was conducted by Wang *et al.*[105] In this study, the experiment was used to assess the accuracy of the proposed matched-field processing (MFP) for leak localization in viscoelastic pipes. It was found that including viscoelasticity and using more frequency in leak localization increased the accuracy of the method. Additionally, the proposed MFP method outperformed the classical leak detection method even for a small leak in a very noisy environment.

d. University of Perugia (Perugia, Italy). Meniconi *et al.*[14] carried out three experiments on the water hammer in a viscoelastic pipe with three different boundary conditions to study the effect of the in-line valve. A partial in-line valve was found to affect both local head loss and differential initial pressure regime, affecting the pressure peak damping in the system.

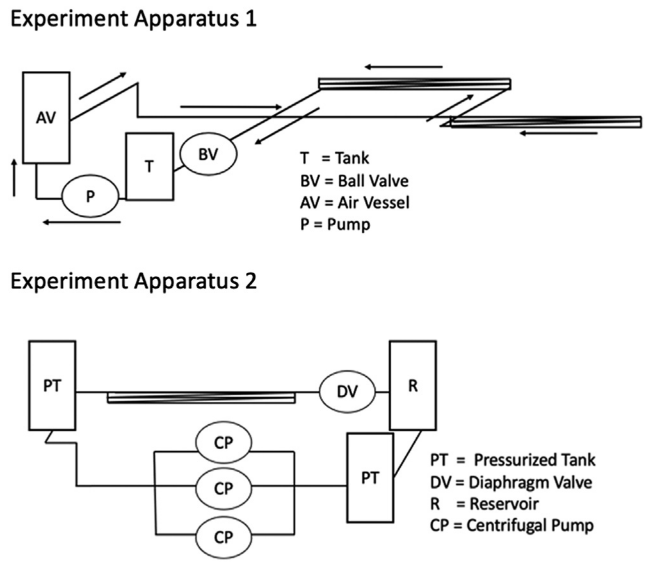

FIG. 14. Experiments conducted at the Instituto Superior Técnico.

e. Shahid Chamran University of Ahvaz. Keramat *et al.*[106] conducted an experiment in a viscoelastic pipeline with six anchoring configurations to investigate the impact of support conditions on the pressure variation in the time and frequency domain. Support stiffness and location were found to influence the pressure variation in the time history. Similarly, changing the support condition modified the resonant frequencies when analyzed in the frequency domain. This finding presented a prospective use of an inverse analysis to determine the support condition.

Another experiment at the Shahid Chamran University of Ahvaz was conducted by Rezapour *et al.*[107] This experiment aimed to assess the performance of Gaussian function-based inverse transient analysis (ITA) for estimating the leak size and location with varying flow regimes, sample size, noise condition, and leak parameters.

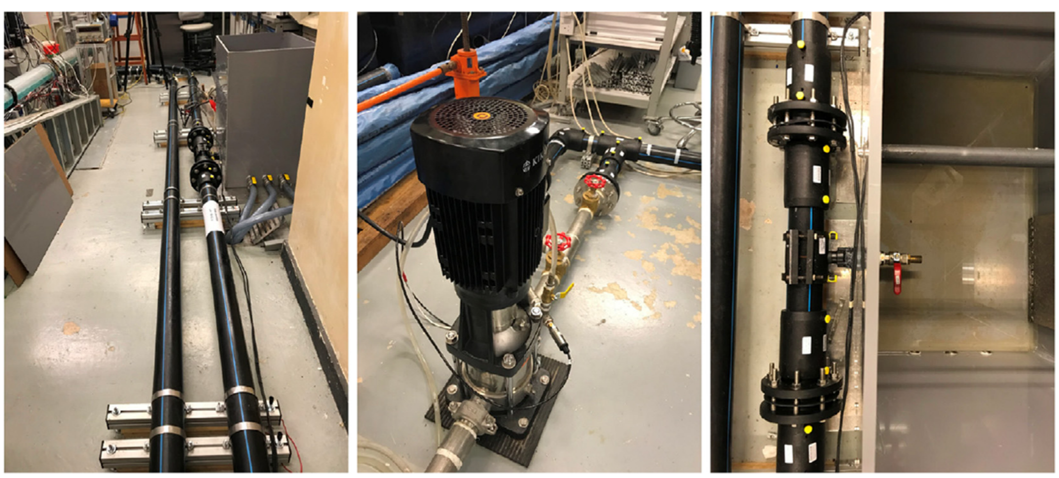

FIG. 15. Apparatus at the Hong Kong University of Science and Technology.

The adopted ITA could predict the leak size and location with simultaneous leak and creep function calibration. For this method, the optimum sample size was half-period of pressure signal for leak location estimation and single period of pressure signal for leak size determination. This method could also be applied for multiple leaks. The two experiments conducted at Shahid Chamran University are displayed in Fig. 16.

f. Other Laboratory Experiments. Other experimental studies on the water hammer in viscoelastic pipes were also performed by Warda *et al.*,[108] Apollonio *et al.*,[109] and Carriço *et al.*[110] on the general water hammer phenomena and calibration of viscoelastic parameters, Soares *et al.*[72,73] on cavitating behavior, Ferrante and Caponi,[18] and Ferras *et al.*[111] on the effect of different pipe materials, and Warda *et al.*[112] on pipe leakage.

2. Pipe networks

a. University of Cassino. Pipe networks consist of pipes arranged in series, parallel, or a combination of the two. An example of the combined configuration of pipes in series and parallel can be seen in a Y-shaped system of HDPE pipes, as investigated by Apollonio *et al.*[113] The main objective of the study was to investigate the effect of constrained and unconstrained junctions in the system simulated by a movable anchor system. From the experiment, a lower peak pressure was found in the case of an unconstrained junction. This showed a different trend when compared to the result in the literature for elastic pipe by Wood and Chao.[114] This discrepancy in tendency may be caused by the additional pressure damping attributed to the viscoelasticity of the pipe wall.

Similar to Apollonio *et al.*,[113] Evangelista *et al.*[115] also conducted a water hammer experiment in Y-shaped branched HDPE pipe systems, but with a focus on wave propagation and reflection. Huge variation was observed between wave propagation and reflection in the experiment when contrasted with the values of classical water hammer. However, a strong agreement was found between the experimental result and the numerical viscoelastic model, which included the effect of unsteady friction and material viscoelasticity. The experiments of the University of Cassino are depicted in Fig. 17.

b. University of Perugia (Perugia, Italy). Despite the foregoing experiments on a single pipe at the University of Perugia, other experiments in a Y-system,[116,117] and more importantly, recently on looped HDPE pipe networks, have been carried out.[118,119]

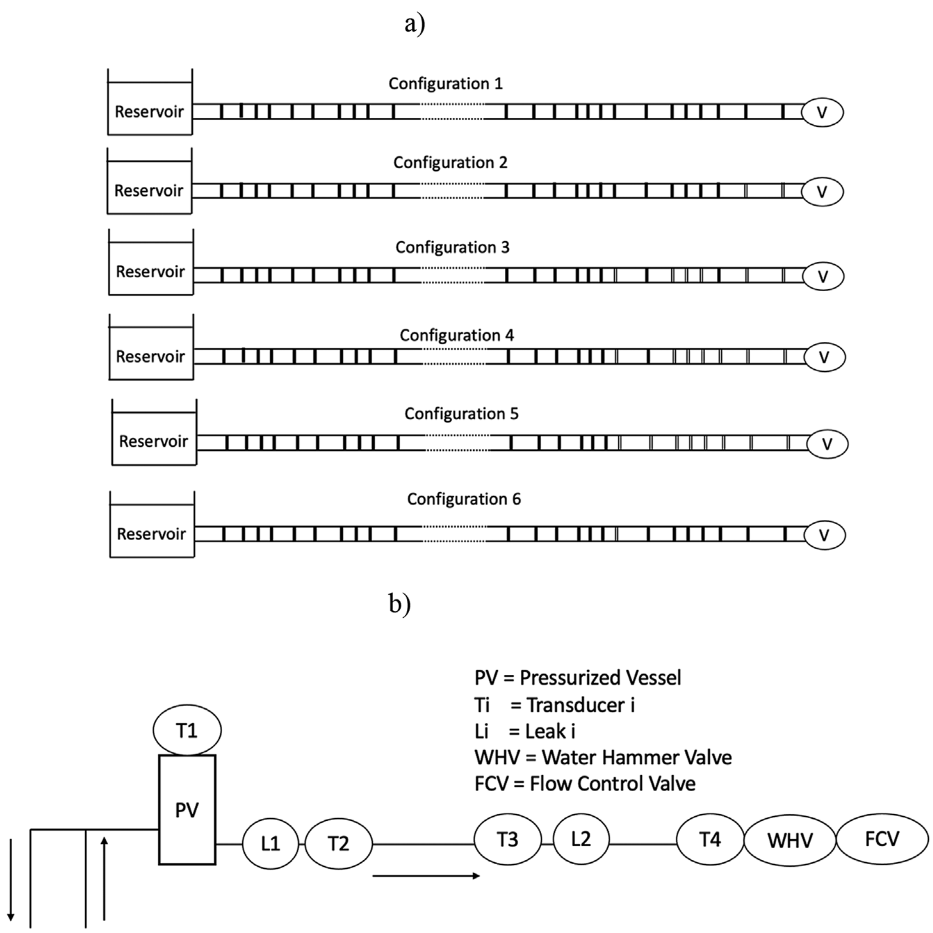

FIG. 16. Experiments conducted with regard to (a) different support conditions and (b) leakage estimation at the Shahid Chamran University of Ahvaz.

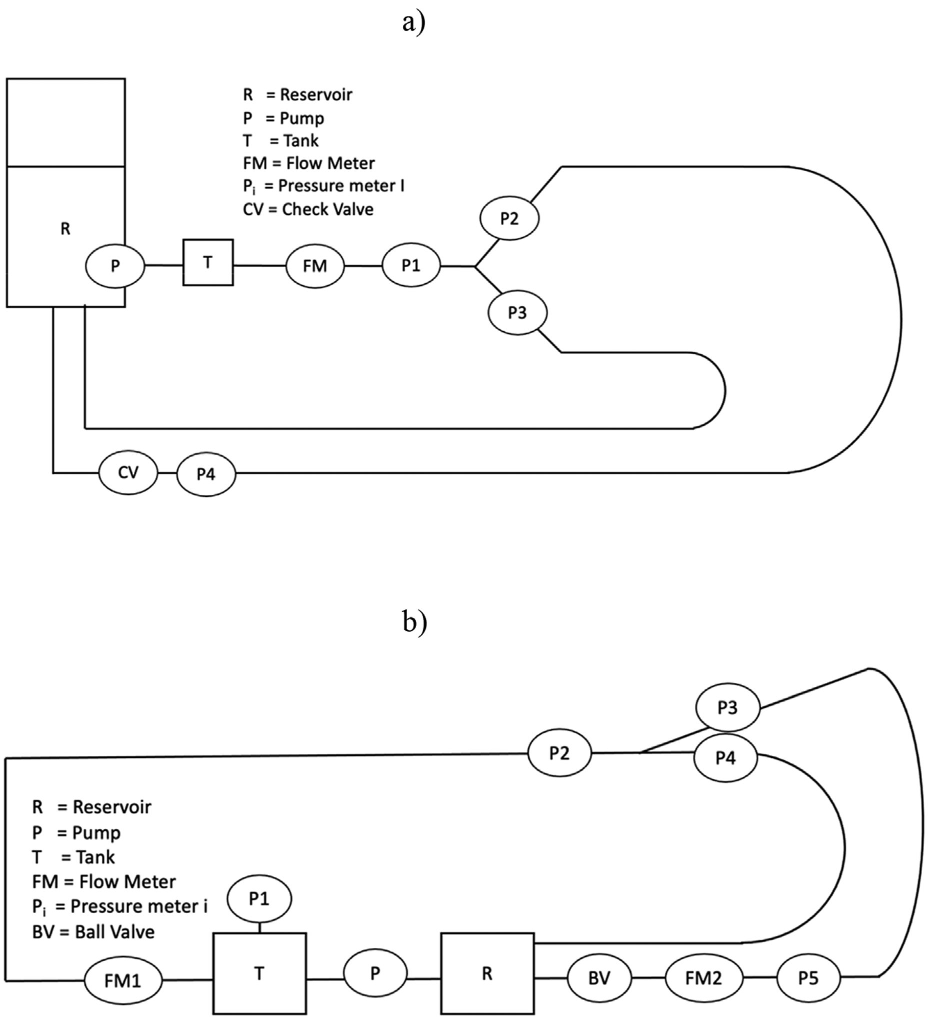

FIG. 17. Experimental apparatus on branched pipelines (a) to study the effect of constraint in junction and (b) wave propagation in branched pipeline.

Another experiment on the branched HDPE pipe system was carried out by Ferrante and Capponi,[116] but with the emphasis on viscoelastic parameter calibration. Viscoelastic calibration was carried out with the same and different numbers of KV elements for all branches. It was then found that calibration with the same number of elements for all branches performed better when compared to different KV elements. Meniconi *et al.*[120] performed another study on the influence of different boundary conditions during transient behavior in four HDPE pipe configurations. The studied pipe networks consisted of pipes with different dimensions, pipe network with a partial blockage, pipe network with an in-line valve, and single pipe. Sudden change in geometry was found to have little effect on pressure signal variation. However, in both in-line valve and partial blockage, pressure variation due to steady-state head loss was observed, with a higher magnitude in the partial blockage case.

Similar to Meniconi *et al.*,[120] Massari *et al.*[121] also conducted an experiment related to the partial blockage in viscoelastic pipes, but it was used to validate the stochastic linear estimator (SLE) in blockage detection. From the experiment, sufficient estimation of blockage geometry, including the blockage size and location, was found, making SLE a prospective future blockage detection method. The experiments conducted at the University of Perugia are represented in Fig. 18.

c. Shahid Chamran University of Ahvaz. Another laboratory experiment on pipe systems was conducted by Fathi-Moghadam and Kiani,[122] as seen in Fig. 19. The experimental apparatus was a 3×3 m polyethylene pipe square loop, and an inverse transient analysis was performed to calibrate the pipes in the network. Overall, the experimental result showed high conformity with the result from an inverse transient analysis. It was also found that by calibrating according to the experimental data of a long pipeline, favorable VE properties could be obtained for complex pipe networks.

Generally, laboratory experiments in pipe networks were conducted mostly with a focus on the boundary conditions and discrete points, such as branched junctions by Apollonio *et al.*,[113] Evangelista *et al.*,[115] and Ferrante and Capponi;[116,120] partial blockages by Meniconi *et al.*[120] and Massari *et al.*;[121] and partial in-line valve by Meniconi.[14] Several experimental studies were also found to contribute

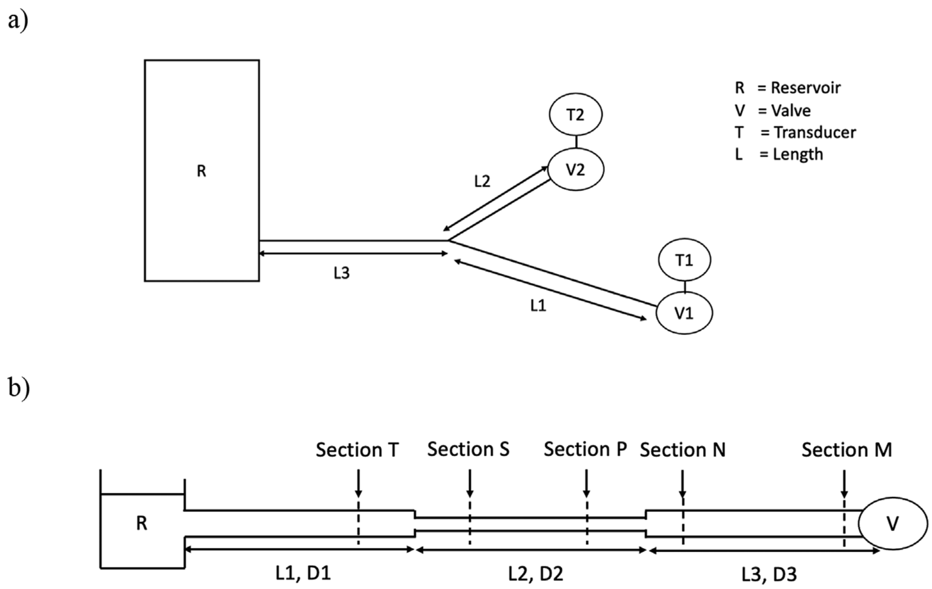

FIG. 18. Examples of the experimental apparatus on the University of Perugia: (a) branched pipe system and (b) a pipeline with blockage.

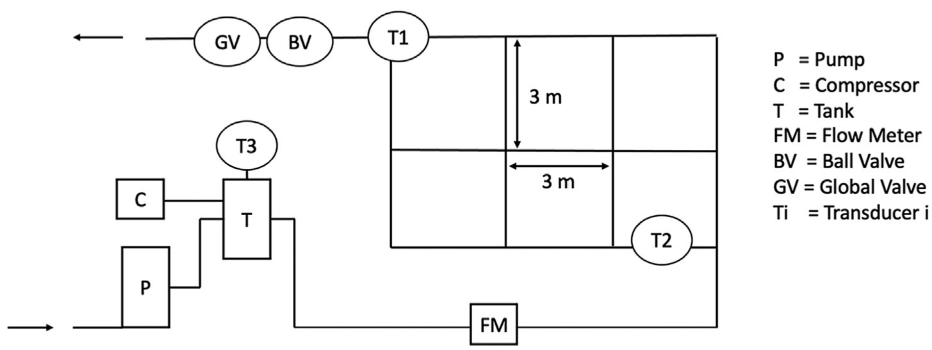

FIG. 19. Experimental apparatus to validate inverse transient analysis.

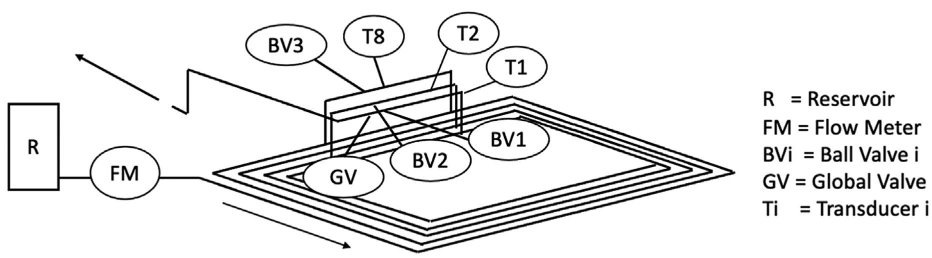

FIG. 20. Field test at Thames Water Facility.

to the validation of numerical methods or calibration of viscoelastic parameters, such as those performed by Massari *et al.*,[121] Ferrante and Capponi,[116] and Fathi-Moghadam and Kiani.[122]

B. Field test

1. Single pipe

a. Thames Water Facility. Covas *et al.*[123] performed a field test of a 1.3-km medium-density polyethylene (MDPE) pipeline, refer to Fig. 20. During the experiment, a secondary transient wave was observed in the experimental system due to check valve closure. It was also found that decreasing the pipeline's diameter size induced pressure signal reflection, increasing the peak pressure experienced in the system.

b. Deltares, Delft. Bergant *et al.*[124] also investigated the effect of viscoelasticity toward pressure variation due to water hammer through a field test. The experiment was conducted in Deltares, Delft, in a

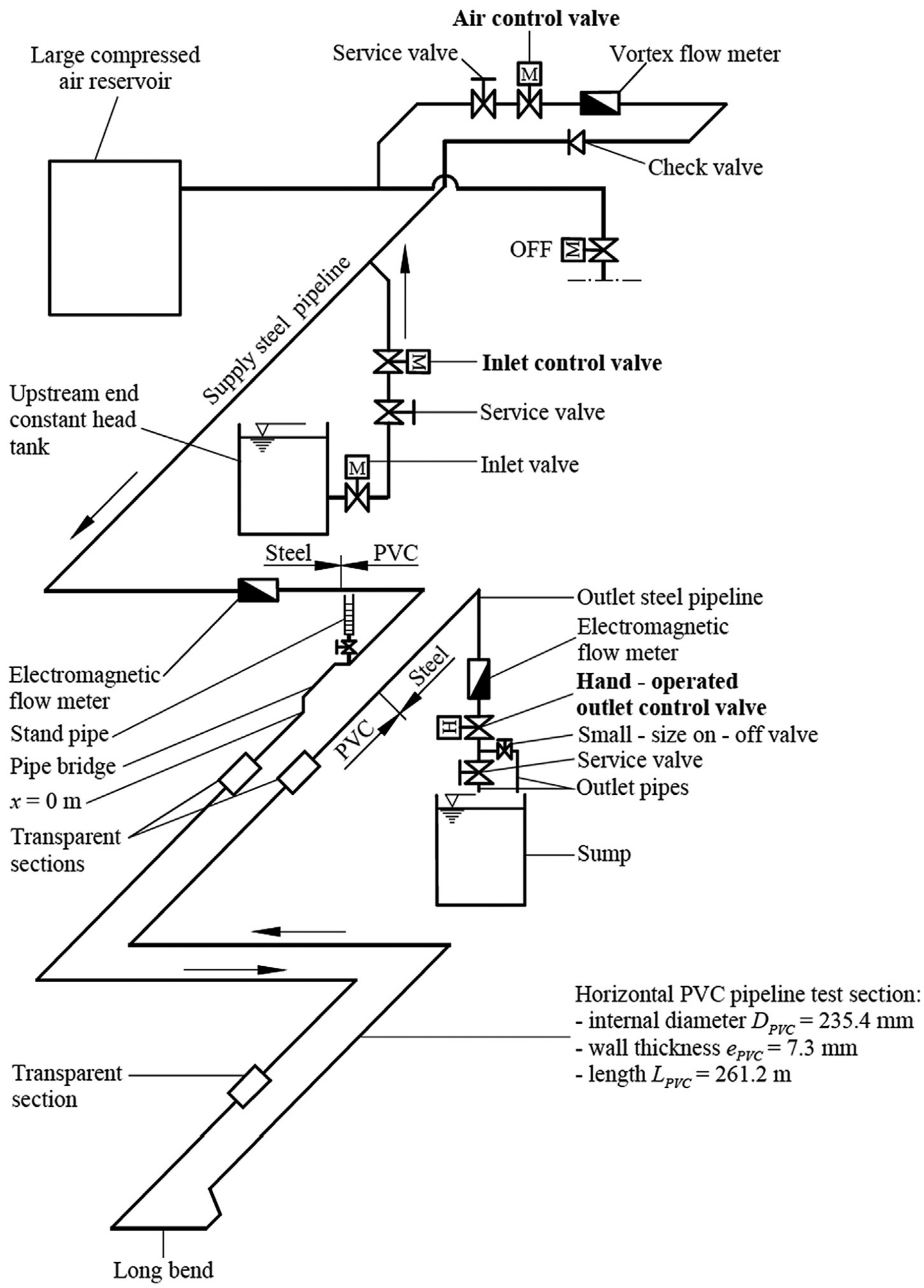

FIG. 21. Field experiment at Deltares, Delft.[124,125] From Bergant *et al.*, "Experimental and numerical analysis of water hammer in a large-scale PVC pipeline apparatus," in 4th International Meeting on Cavitation and Dynamic Problems in Hydraulic Machinery and Systems. Copyright 2011. Reproduced with permission from A.K.

large-scale PVC pipeline, as seen in Fig. 21. The experimental result was compared with the numerical model, and it was found that the experimental result displayed high compliance with the numerical model, which incorporated unsteady friction and pipe wall viscoelasticity.

The previous experimental arrangement was then improved by Bergant *et al.*[125] by ensuring a constant upstream head leading to a simplified numerical simulation and fewer boundary condition-related calibration flaws. With this improvement, other factors contributing to dynamic effects could also be identified, including some significant dynamic effects due to the influence of short steel pipes, FSI, and unsteady friction. Other dynamics effects such as non-linear viscoelastic effect, pipe-rack vibration, pipe wall thickness, convective terms, and cavitation could also influence the pressure variation during transients.

c. San Louis Potosi, Mexico. Carmona-Paredes *et al.*[33] conducted another field experiment to verify the proposed numerical simulation

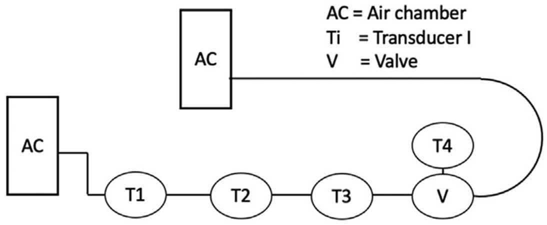

FIG. 22. A field experiment conducted in San Louis Potosi.

of transients in HDPE pipes through a standard solid model. High agreement was then found between the experimental result and the proposed modeling of HDPE behavior, validating the use of the standard solid model. The experiment apparatus at San Louis Potosi is displayed in Fig. 22.

2. Pipe networks

a. Balmashanner Pipeline. Ramos and Covas conducted a real-life test on a branched pipe system in Balmashanner of 5940-m-long pipe made from buried ductile steel materials,[104] seen in Fig. 23. The main contribution of this study was to determine the significant dynamic effect in the system and validate the use of appropriate numerical modeling. From the study, it was found that unsteady friction was the major dynamic effect in the system. The application of the MOC-based model, which incorporated unsteady friction, provided reasonable results in terms of accuracy, efficiency, and robustness.

b. Willunga Pipeline Network. Another field test on pipe networks was performed by Stephens *et al.*[126] This study aimed to investigate the inaccuracies of transient pressure estimation in the Willunga water distribution network. Willunga water network consisted of two loops with multiple branches of 100- to 150-mm-diameter asbestos cement pipes with a total length of approximately 4 km. This water network was separated from the surrounding water networks by closed valves (isolation valves) and the Willunga tank, as shown in Fig. 24. Within the experiment, two transient generators were installed with three stations for pressure monitoring. Fire plugs, with a quantity of approximately 50, were well-distributed throughout the extent of the Willunga water network. The testing result was compared with different numerical modeling means, such as quasi-steady friction, unsteady friction, and damping-based model. It was then found that the numerical simulation with damping represented by the Kelvin–Voight elements was the most suitable in predicting the field results as it incorporated mechanical pipe properties and joint interaction and vibration along with the energy transfer in the system.

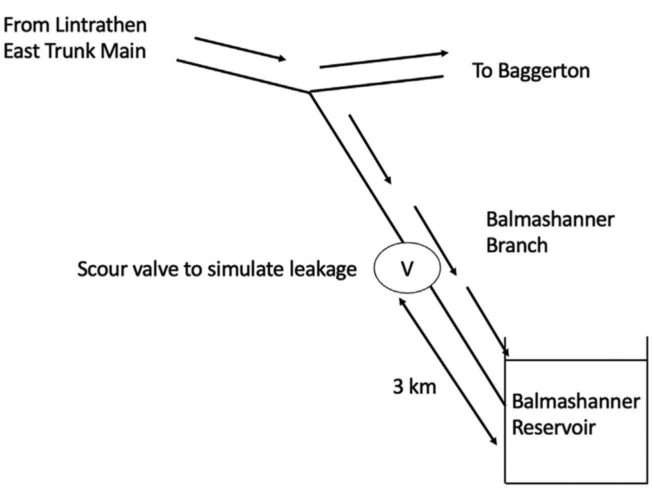

FIG. 23. A field experiment in Balmashanner Pipeline.

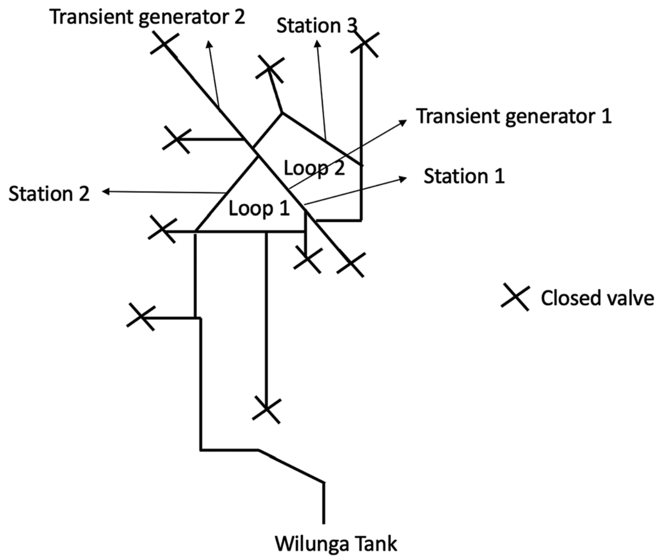

FIG. 24. Field test on Willunga Network.

Overall, the current number of field network testing is relatively limited compared to other experimental studies, such as laboratory testing for single and pipe networks or field tests for a single pipe. The lack of field study on pipe networks is possibly due to the less ideal result contributed by *in situ* conditions and scale-induced complications arising from the temporary isolation of the pipe network. Despite these drawbacks, field study on pipe networks is still necessary to measure the gap between the idealized plan and real-life conditions.

V. NUMERICAL ANALYSIS IN THE TIME-DOMAIN

The most straightforward solution approach is referred to as the time-domain analysis, which allows for investigating the variation of pressure or head and flow rate during water hammer with time.[6] In this analysis method, the continuity and momentum equations of the transient system are solved using computational methods with time and space (longitudinal direction of the pipe) as the independent variables. Likewise, the boundary conditions and nonlinear effects (such as viscoelasticity, unsteady friction, cavitation, and other effects), which are presented as mathematical expressions, are combined with the other computational expressions in the solution process. Specifically, for the time-domain numerical implementation, the resulting expressions stemming from the viscoelasticity behavior, which are in the form of convolution integrals, are first approximated and then used to find the response at each time step by computer programming. To date, there is a wide range of tools for the analysis in the time domain, starting from the method of characteristics (MOC), which is the most consistent with wave physics, to the smoothed particle method (SPM), being blind to the physics of the propagating waves. In this segment, the numerical schemes implemented in viscoelastic pipes are elaborated.

A. The approximation of the convolution integrals

Convolution integrals in the mathematical model exist in the continuity and momentum equation to represent viscoelasticity and unsteady friction, respectively. To estimate the convolution integral corresponding to the viscoelastic effect, Covas *et al.*[9] and later Keramat *et al.*[3] proposed a recursive numerical scheme that evaluated the integral according to the pressure at previous and current time steps. Afterward, Wienerowska-Bords used the non-dissipative Preissmann scheme, which was a four-point scheme finite-difference method (also known as box scheme).[127] Application of the non-dissipative Preissmann scheme was found to eliminate the numerical diffusion error, showing better results in terms of physical damping and smoothening.

In the momentum equation, Franke and Seyler estimated the convolution term by the impulse-response method (IRM).[128] Another approach was to adopt an effective weighting function approximation[53–57] as described in Sec. III C.

B. Method of characteristics (MOC)

MOC is the most commonly adopted numerical solution for the water hammer in viscoelastic pipes. In MOC, partial differential equations are converted into ordinary differential equations along different characteristic lines, which can then be solved by a simple finite difference scheme.[110,129] The main advantage of MOC is the programming simplicity and computation efficiency.[110] MOC also perfectly represents the essence of transient flow, which is characterized by fast convergence with high calculation accuracy.[130] Despite its strength, MOC is relatively less robust for complex pipeline configurations such as cross-sectional change or flexible pipeline material. While problem-solving in the previous case is still possible, MOC is not applicable in a simple way, and rearrangement of the programing code is necessary, making other methods, such as finite volume, a preferable alternative.[131]

Over the years, MOC has also been applied to obtain the numerical solution for water hammer in viscoelastic behavior with dynamic effects such as unsteady friction,[3,13,104,132] FSI,[3,97,100–102] cavitation,[3,83,86] leakage,[112,133] and blockage.[134]

C. Wave characteristics method

The wave characteristics method is formulated based on Newton's second law to accurately model the physical behavior of fluid flow in the system. Despite the method's early establishment by Wood *et al.*[135] for elastic pipes, this method is still relatively new for water hammer in viscoelastic pipes. To the author's knowledge, the only application of the wave characteristics method in the viscoelastic pipe was by Abdel-Gawad and Djebedjian.[136] When compared to other computational methods such as MOC or finite volume method, the wave characteristics method was capable of performing a better estimation of transient pressure variation with the same computational effort.

D. Godunov method

Other than the previous methods, Seck proposed another method by the Godunov finite volume method.[137] This method solved PDE in CFD by considering the conservation laws within a finite volume. This research was an extension of the previous study on Godunov finite volume by Seck *et al.*,[138] which was devised for elastic pipes. Compared to the previous study, an additional source term was included in the mass conservation to represent the mass flux in the radial direction. The applied method could satisfactorily predict transient pressure in viscoelastic pipes with a relatively short computational time, making it an effective qualitative analysis tool.

In a recent study, Ning *et al.*[139] applied the second-order Godunov finite volume method to solve the numerical model considering column separation in viscoelastic pipes during the transient occurrence. The result calculated based on the second-order Godunov finite volume method was more accurate than the traditional MOC method when the Courant number of less than one was adopted.

The time-domain analysis is relatively more popular than the frequency-domain analysis for viscoelastic pipelines due to a better representation of the retarded behavior, leading to a better understanding of viscoelasticity. However, with higher modeling accuracy, the analysis in the time domain becomes more complicated, requiring higher computational time and effort. Other than modeling significance, the time-domain analysis has also been used in viscoelastic pipes, including blockage and leakage, as explained in Sec. VIII.

VI. FREQUENCY-DOMAIN ANALYSIS

Transient flow is a frequency-dependent phenomenon. The various dynamic effects (unsteady friction or viscoelasticity) impact the transient properties over time, thus distorting the contribution of different frequencies. The frequency-domain or spectral analysis captures the frequency content of the state variables by which the variation of pressure or flow rate with different frequencies is studied. Analyzing transient behavior in the frequency domain helps observe the relevant dynamic effect and its influence on the variation of frequency.[140] Frequency-domain analysis transforms the continuity and momentum equations from the time domain to the frequency domain using the Fourier or Laplace transforms. Each transformed equation has a linear relationship, which is then superpositioned to obtain the system response function. In elastic pipes, two methods for the frequency-domain analysis include the impedance method and the transfer matrix method (TMM).[6] These methods are applicable even for viscoelastic pipes due to the favorable presentation of the convolution integrals in the frequency domain.

The impedance method was adopted by Covas *et al.*[141] to develop the impulse response method (IRM), which considered both frequency-dependent friction and wave speed. In this method, transfer functions of the system based on constitutive equations were determined as a function of impedance, evaluated by inverse Fourier transform (IFT), and calculated by convolution to obtain transient pressure response. This method was relatively much faster compared to the time-domain method, such as MOC, with easier inclusion of frequency-dependent factors. However, loss of accuracy may be encountered due to the linearization of non-linear effects. To minimize the discrepancy between the impedance method with time-domain methods, Capponi *et al.*[142] proposed a more accurate linearization for the frictional effect along with a correction factor based on parameter analysis between the impedance method and the method of characteristics (MOC). When an optimal correction factor was applied, the impedance method could produce a comparable result to MOC.

Similar to the impedance method, the transfer matrix method (TMM) is also based on the linearization of continuity and momentum equation. While the impedance method and TMM are similar in concept, TMM is preferred for the frequency-domain analysis of complex pipelines. TMM is relatively simpler and more systematic than the impedance method, yielding superior results for complex systems with irregularities. One of the earliest applications of TMM in viscoelastic pipes was by Duan *et al.*[16] The frequency response function method (FRFM) for VE pipes was derived with a similar form to the transfer matrix by Lee *et al.*[143] and Chaudhry[6] for elastic pipes but with different matrix coefficients. In recent developments, TMM has also been modified for viscoelastic pipes to incorporate FSI,[99] FSI-leakage coupled effect,[144] leakage,[16,145] and blockage.[146]

VII. CALIBRATION OF THE VISCOELASTIC PARAMETERS

Calibration is the process of adjusting parameters in the model such that the simulated system behaves similarly to the real-life system. For the case of transients in viscoelastic pipes, the calibrated parameters include valve parameters, pipe wall roughness, wave speed, unsteady friction coefficient, retardation times, and creep compliances. While some of these parameters can be evaluated via deterministic formula, the retardation times and creep compliances, referred to as the VE parameters, usually are found by optimization. The calibrations in early research consider constant quantities as the retardation times so that optimization is executed to find the compliances only.[9] However, recent applications suggest the simultaneous calibration of the retardation times and creep compliances to arrive at more accurate coefficients.[105,147] Several aspects affecting the calibration of viscoelastic parameters, such as the different number of KV elements, optimization algorithms, stepwise method, time domain, and frequency domain calibration, are elaborated here.

A. Optimization method

The optimization calibration method is applicable when the measured transient data are available. For the one and two KV element models, calibration can be performed by either trial-and-error or optimization methods. However, for more KV elements, with a higher number of data, an efficient optimization method is preferred.[148] Typically, in the optimization process, the main objective is to minimize the error between experimental measurement and simulation results by finding optimum model parameters.

The most frequently adopted optimization algorithm in the literature for calibrating the VE parameters is implemented by the genetic algorithm.[123,149,150] A subset of this algorithm called the microgenetic algorithm, which is essentially a genetic algorithm but applied on a smaller scale, has also been applied.[11,151] Other applied algorithms include the Levenberg–Marquardt algorithm,[149,150] and the shuffled complex evolution of the University of Arizona (SCE-UA).[131]

B. Number of KV elements

The number of KV elements in the system determines the accuracy of the viscoelastic calibration. With more KV elements, higher calibration accuracy can be achieved.[152,153] However, less improvement in performance is found for larger than four KV elements,[9] with the 5-elements model being satisfactory for most viscoelastic materials.[154] For branched pipe systems, applying the same number of KV elements for all branches produces better results when compared to different KV elements.[116]

C. Stepwise method

While the optimization method may be efficient, errors may arise due to inaccurate transient solver and determination of parameters with similar influences. In response to the weakness of the optimization method, Carriço *et al.*[110] proposed a two-staged calibration approach with stage one for the calibration of steady-state and stage two for the determination of transient-state parameters. Stepwise calibration was found to show excellent conformity between numerical and measured data, thereby accurately describing viscoelastic behavior during a transient. The framework of stepwise calibration by Carriço *et al.*[110] is displayed in Fig. 25.

D. Time-domain calibration

One method to calibrate in the time domain is called the inverse transient analysis (ITA). In ITA, a rapid transient occurrence is first simulated in a pipeline system in which the pressure data are collected. Then, a numerical model is developed for transient behavior in viscoelastic pipes. In the calibration process, the difference between the numerical model and the experimental result is minimized with the help of optimization tools by changing the viscoelastic parameters: creep function (J_k) and retarded time (τ_k).

The first researcher to apply ITA for the calibration of viscoelastic pipes was Covas *et al.*[123] Viscoelastic calibration based on ITA was found to produce high conformity between numerical simulation and experimental results. However, this study by Covas *et al.*[123] failed to distinguish the effect between pipe wall viscoelasticity and unsteady friction, which both had dissipative effects toward transient. This issue was then solved by Soares *et al.*,[150] who modified the calibration steps. First, the wave speed was calibrated to account for unsteady friction behavior. Then, viscoelastic parameters were obtained from the viscoelastic transient solver without considering the unsteady friction behavior, which had been determined previously. This calibration method successfully isolated the effect of viscoelasticity and unsteady friction, which was the weakness of the previous study by Covas *et al.*[111] Other than viscoelastic calibration, in recent years, ITA has also been applied to detect leaks in pipelines, which will be further elaborated in Sec. VIII B.

Keramat and Haghighi introduced another time-domain calibration tool specifically used for a relatively long viscoelastic pipe.[17] The creep parameters were determined based on the approximate solution of the mathematical model, offering explicit formula for the pressure

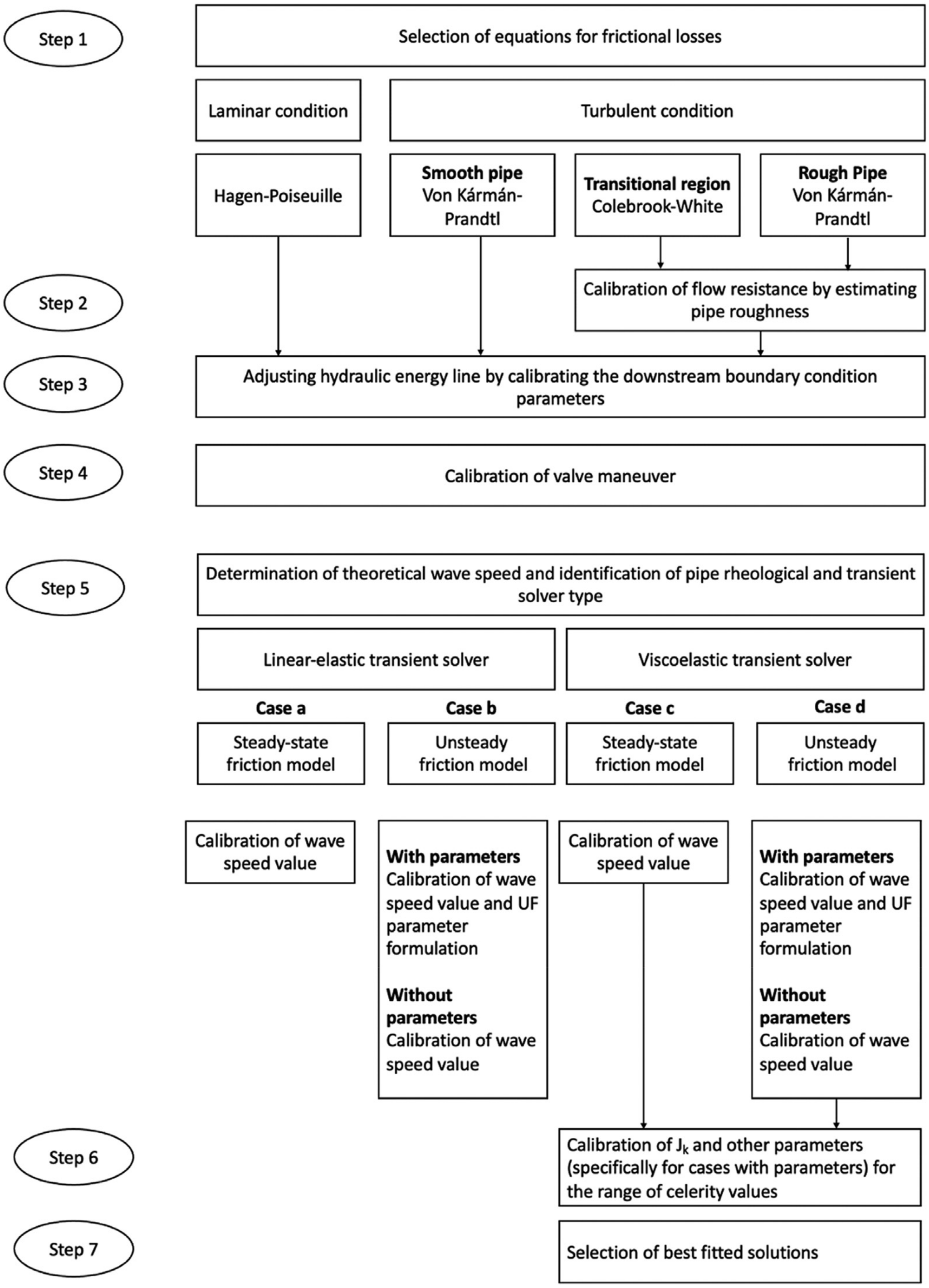

FIG. 25. Stepwise calibration procedure for viscoelastic parameters.

head variation during the first half period of a transient. This method was relatively easier to apply compared to other methods, with fewer experimental data leading to less uncertainty and measurement error. Additionally, as this method utilized only the first-half period, this method did not require heavy numerical computations. However, this method was applicable only for a relatively long pipe to ensure the functioning of all KV elements during the concerning first-half period.

E. Frequency-domain calibration

Frequency-domain calibration may be better than the time-domain when the time variation over a long duration is of interest.[152] In recent years, several calibration methods in the frequency domain have been formulated. Gong *et al.*[155] proposed a frequency-based viscoelastic calibration by using a frequency response diagram (FRD) to obtain elastic wave speed and viscoelastic compliance of the pipeline. The viscoelastic parameter was corrected to account for frequency variation induced by unsteady friction. Despite providing satisfactory accuracy for both elastic wave speed and viscoelastic parameters, practical complications may arise regarding the selection of retardation time, influence of resonant frequency, and complexities in real pipelines.

Another frequency-based calibration method was suggested by Pan *et al.*[147] with the use of a multi-staged frequent-domain transient-based method (FDTBM). First, the creep compliance and retarded time were obtained for the single-element KV model. Adopting the previous parameters to a two-element KV model by FDTBM, viscoelastic parameters for the second KV element were determined and then extended for the three- and four-element KV models. Calibration of viscoelastic parameters with multi-staged FDTBM was found to provide unique and accurate viscoelastic parameters for most cases, but the applicability and accuracy may vary depending on the viscoelastic parameter and the pipe scales.

VIII. DEFECT DETECTION

A. Blockage detection

Blockage limits fluid flow in pipes, preventing pipes from performing their intended purpose. Considering the disturbances it causes, methods shall be formulated to detect and characterize blockage, including the location, size, and extent of the blockage. Generally, there are two types of blockage depending on the blockage size relative to the pipe length: discrete blockage and extended blockage. Discrete blockage covers a relatively shorter distance compared to extended blockage and can be analyzed as a single discontinuity point.[156] In the blockage detection process, the extended blockage detection method may not be applicable for discrete blockage detection and vice versa, even though in recent years, universal blockage detection tools, capable of detecting both discrete and extended blockage methods, have been proposed.[157] In this segment, only blockage detection tools that have been applied in the viscoelastic pipeline are further elaborated.

Duan *et al.*[146] proposed an extended blockage detection method based on the frequency response analysis (FRA). In FRA, the water hammer model was first formulated and transformed by TMM, as described in Sec. VI, to obtain the frequency response, which was then validated by experimental data. The extended blockage induced shifts in the transient resonant frequency, as shown in Fig. 26. By analyzing the frequency response, the blockage properties, including the extent and size, could be estimated. However, viscoelasticity also induced shifting in peak resonance. Resonance shift due to the VE effect was relatively monotonic and could be obtained by applying the analytical formula by Duan *et al.*[146] with prior knowledge of the viscoelastic parameters. For this method to be applied in the viscoelastic case, the resonance shift from viscoelasticity shall first be isolated from the resonance shift due to extended blockage before analyzing the system's frequency response to obtain the blockage parameters.

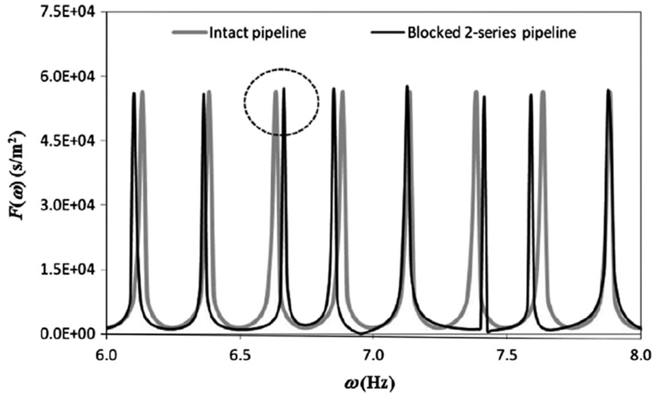

FIG. 26. Comparison between the frequency response of intact and blocked pipeline.[146]

Another blockage detection method, applicable for both discrete and extended blockage, was suggested by Meniconi *et al.*[158] Meniconi *et al.* combined the frequency domain (FRA) proposed by Duan *et al.*[146] and the time-domain method, which was the pressure signal analysis (PSA). In PSA, the pressure head was observed over time, as the pressure head increased with the existence of blockages. Based on the time of the pressure rise (the wave travel time), the location of the blockage could then be estimated. PSA was superior in terms of estimating the blockage location, while FRA had its advantage in terms of estimating the geometry of the blockage, as previously elaborated. To produce the most efficient result, PSA was first applied to estimate the blockage location, and FRA was then applied to find the geometry. In the viscoelastic pipe, several modifications were performed. PSA shall also consider the pressure decay due to pipe wall viscoelasticity as performed by Meniconi *et al.*,[159] while FRA shall be performed similarly to FRA analysis of blockage for viscoelastic pipe as performed by Duan *et al.*[146] While this method was found to perform better compared to PSA or FRA method, this coupled method was more accurate in elastic pipes in comparison with the viscoelastic pipes.

Massari *et al.*[160] utilized a stochastic method called successive linear estimator (SLE), typically used in groundwater hydrology, to estimate extended partial blockage in the viscoelastic pipe. Viscoelasticity was included in the formulation of the forward model and then calibrated based on one single-diameter representative pipe. SLE, as an inverse model, was then applied to estimate diameter based on pressure variation collected from the experiment. While this method can be applied to detect blockage in simple pipelines along with the determination of blockage size and location, errors may still be possible due to cross-sectional change, parameterization error, model structure error, or noise effects.

Another potential blockage detection method was devised by Kumar and Mohaparta.[161] The proposed method utilized a modified reconstructive method of characteristics (MOC) to detect partial discrete and extended blockage based on steady-state pipe pressure head and pipe area reconstruction, respectively. The pipe segment was first separated into finite cells with blockage assumed to be located at the interface of the discretized cells. Characteristics equations were then derived according to the back calculation of steady-state parameters. This method was applicable to both elastic and viscoelastic pipelines.

For the viscoelastic case, the numerical model with pipe wall retarded behavior shall be considered. With this requirement, viscoelastic properties were obtained through calibration in advance before this method was applied. Without the inclusion of viscoelastic properties, significant deviation was observed for both discrete and extended blockage cases when compared with the experimental result. The benefits of this method were the less need for preliminary knowledge of blockage number, upstream boundary condition, friction factor determination for discrete blockage, and regular geometry assumption in extended blockage.

B. Leakage detection

Similar to blockage, leakage is also a disturbance in pipe flow. However, contrary to blockage, which restricts fluid flow and increases fluid pressure, leakage provides an additional flow outlet, decreasing the peak fluid pressure, as seen in Fig. 27, while increasing the wave pressure damping. Typically, pressure damping serves as a unique characteristic to evaluate the leak parameters, such as leak size and location. However, in a leaky viscoelastic pipe, the leak detection problem becomes more complex. Damping behavior is caused by leaks and pipe wall viscoelasticity, which may disguise leak-induced damping. This may reduce the effectiveness of previous leak detection tools for elastic pipes.[145] Modifications shall then be proposed to the existing leak detection tool to be extensible even for viscoelastic pipes. In general, the leak detection methods can be classified into the time-domain or frequency-domain approaches.[162]

1. Time-domain approach

The inverse transient analysis (ITA) is the most commonly adopted time-domain leak detection tool. First proposed by Pudar and Liggett[163] and then modified by many other researchers,[164–167] the ITA is a method to estimate unknown leak parameters based on the collected transient data.[168] Originally developed for elastic pipes, ITA's applicability was extended to the viscoelastic pipe by Ramos and Covas.[149] To find the parameters, the forward transient solver (FTS), a numerical program for the system's pressure variation with leaks, was first prepared. FTS shall include not only unsteady friction and other dynamic response such as cavitation but also the viscoelasticity effect for ITA to be applicable for viscoelastic pipes. Then, the solver results were compared with the experimental data to construct an optimization problem. The least-square error then optimized the difference in the inverse transient solver (ITS). The ITA was capable of obtaining leak parameters when the pipeline's physical characteristic was known, the leak was of reasonable size, and an accurate transient solver was used. However, the detection results were sensitive to the sensor location, valve maneuver, pipeline material, and other system configurations.

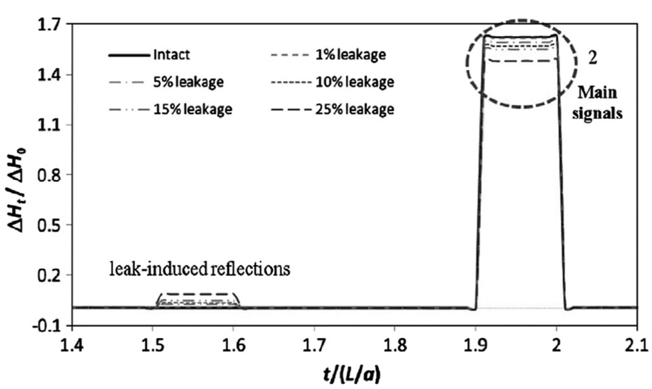

FIG. 27. Variation of pressure head with different leakage degree.[16]

Several modifications in ITA have also been proposed, especially regarding the applied optimization algorithm for viscoelastic pipes. Soares *et al.*[169] utilized a multi-staged optimization algorithm with a coupled optimization method of global optimization (genetic algorithm) and local optimization (Levenberg–Marquardt algorithm), inspired by Kapelan *et al.*[166] approach for the elastic pipes. This optimization procedure was found to improve leak detection performance in terms of detection speed and accuracy. Another algorithm that was applied in conjunction with ITA for the viscoelastic pipe was Nelder–Mead algorithm. Choura *et al.*[170] applied the Nelder–Mead algorithm both in the process of viscoelastic parameter calibration and leak determination of ITA. It was found that adopting Nelder–Mead algorithm produced acceptable viscoelastic calibration and leak detection accuracy.

Mousavifard *et al.*[171] performed another modification of ITA but in the mathematical representation of the viscoelastic pipe. The modification, called backward transient analysis (BTA), was based on a new scheme of MOC in which the transient flow analysis began at the downstream end after the transient was fully developed. In terms of performance, with a bigger leak, BTA had a similar performance to ITA. However, BTA successfully removed the uncertainties in ITA, which was the undesirable effect at the downstream valve, and performed better than ITA, especially in the case of a smaller leak.

Another concern with ITA is the computation cost due to the tedious optimization process. As a solution, Wang proposed substituting the numerical model with an easy-to-compute surrogated model built by modeling transient waves with the Kriging method based on a sparse sampling strategy.[172] This method was found to have similar accuracy to the traditional ITA but with a lower computation cost.

The transient damping method (TDM) is another viable option for leak detection of viscoelastic pipes in the time domain. First derived by Wang *et al.*[173] and Nixon *et al.*,[174] TDM has also been extended to be applicable even for viscoelastic pipes. Brunone *et al.*[175] proposed a decay law approximation of TDM for leak detection in the viscoelastic pipe. First, the numerical model for the viscoelastic pipe was formulated and experimentally calibrated. Then, numerical tests were performed to determine the appropriate decay law coefficients for the corresponding viscoelastic pipes. Peak pressure was found to be a characteristic parameter crucial for the determination of leak location, properties, and pre-transient pressure. On the other hand, initial flow velocity at the downstream location was found to have a negligible effect on the leak detection result.[176] Furthermore, to improve TDM's reliability, Capponi *et al.*[177] proposed the use of TDM coupled with other methods, such as analyzing the pressure signal during the first half-period to obtain the wave reflection information.

2. Frequency domain approach

In the frequency domain, Duan *et al.*[16] proposed a frequency response function (FRF)-based method to detect pipe leakage. First, FRF was derived numerically for elastic pipe and then extended to the viscoelastic case with leakage by the use of TMM. This method was also applied with varying experimental bandwidths. In a more recent study on the same method by Pan *et al.*,[145] bandwidth variation was quantified by delayed timescale (DTS). While this method achieved acceptable leak property accuracy for both size and location, this method was found to be more sensitive to leak location compared to leak size. For this method, the preferable DTS was recommended to be within the characteristics wave timescale.

Matched field processing (MFP), as suggested by Wang *et al.*,[105] is another method to detect leaks in viscoelastic pipes in the frequency domain. In this method, viscoelasticity was first represented by frequency-dependent wave speed. The leak was then localized by the MFP algorithm and applied to search for leaks along the pipeline. The viscoelasticity effect shall be included with the use of more frequencies in the algorithm for better accuracy. MFP was found to be accurate with fast computation, even for a small leak.

Keramat *et al.*[144] also derived an FRF-based tool for leak identification of viscoelastic pipes but including the effect of FSI. Similar to Duan *et al.*[16] and Pan *et al.*,[145] FRF was first derived by TMM but was then exploited by localization through MFP and maximum likelihood estimator (MLE). Consideration of FSI was observed to increase the accuracy of leak identification due to the larger Poisson effect in the viscoelastic pipe.

IX. VISCOELASTICITY IN SURGE CONTROL

The transient phenomenon induces a sudden pressure rise in the pipe system, leading to potential pipe damage. Different surge control methods have then been proposed to address this issue. In recent years, the viscoelastic pipe is becoming a more prospective surge control method due to its damping characteristics, which ultimately leads to lower peak pressure. By including viscoelastic pipes into the existing piping system through different configurations, peak pressure in the system can be significantly reduced, providing maintenance-free surge control tools compared to the conventional methods.[178]

In 1999, Tijsseling *et al.* installed an internal rectangular tube made of different materials to reduce the impact of water hammer, especially regarding the pressure wave speed.[179] Both steel and PVC tubes could successfully achieve this. However, PVC internal tube produced better results as it displayed a beneficial damping behavior in addition to the decreased pressure wave speed. Despite PVC's superior performance, the use of steel tubes was still more recommended compared to the PVC tube, as the successful application of this method was highly dependent on the material's strength.

Viscoelastic pipe's potential as a surge control method only gained more recognition after the proposition by Triki.[178] Triki suggested substituting a short region in the pipe system, highly critical to transient pressure rise, with a short in-line polymeric pipe of either low-density polyethylene pipe (LDPE) or high-density polyethylene pipe (HDPE). This method was found to induce a lower peak pressure during transients. Between HDPE and LDPE, the use of LDPE provided better damping behavior compared to HDPE. Additionally, the volume pipe section also affected the damping in the pipe system. The application of a short in-line polymeric section as a surge control measure is shown in Fig. 28.

Triki then suggested a similar method but using a branched polymeric penstock instead of an in-line polymeric section.[180] A branched polymeric penstock was also capable of mitigating the excessive pressure peak experienced by the pipes. Similar to Triki,[178] more deformable pipes were also found to improve damping performance. When compared between branched polymeric penstock and in-line polymeric section, a branched polymeric penstock had an increased small period rate with relatively easier implementation. The viscoelastic-based transient control measure with branched polymeric penstock is depicted in Fig. 29.

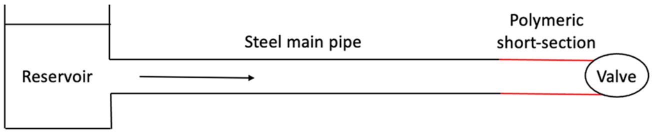

FIG. 28. Adaptation of short in-line polymeric section control method.

Triki analyzed the performance of the previous in-line control method with two additional characteristics: circumferential stress and radial strain.[181] While the in-line method displayed good pressure head results, this method produced some unfavorable effects, such as amplification of radial strain, and caused a delay in the steady-state regime. It was then suggested that these two aspects were assessed as two additional design criteria in addition to pressure head damping.

Another method for surge control was proposed by Triki.[182] The newly proposed dual method replaced two parts of the pipeline, which were the upstream and downstream locations, with two short polymeric sections. Compared to the traditional in-line method, the dual method limited the delay in steady-state and amplification of radial strain, producing a better surge control mechanism. From this study, the application of the dual method was found to produce the best setup with an acceptable trade-off between pressure damping, amplification of radial strain, and delay in the steady-state regime.

Similarly, Trabelsi and Triki adopted the dual method but replaced the two parts with two branched polymeric penstocks of different materials,[183] as shown in Fig. 30. In this study, HDPE and LDPE branched penstock was located at the passive hydraulic region and transient sensitive region. This method was also found to produce a better trade-off between pressure damping, radial strain amplification, and wave oscillation spreading compared to the conventional branching method.

Triki and Trablesi proposed another arrangement of the dual method with the combined use of in-series and branched penstock,[184] refer to Fig. 31. This method was also found to provide an advantage over conventional in-line or branched methods in terms of peak pressure head and pressure wave oscillation. Comparing the pipe materials, adopting the combined dual method based on LDPE pipes yielded better results compared to HDPE pipes.

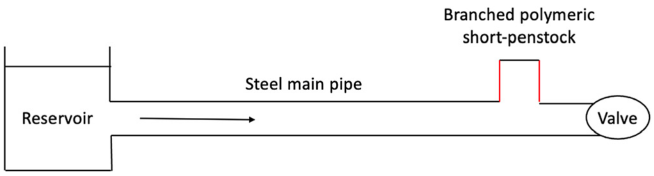

FIG. 29. Surge control with a branched polymeric penstock.

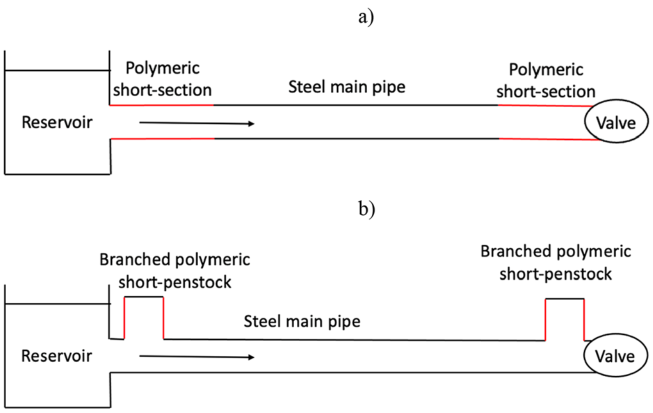

FIG. 30. Application of dual technique by (a) inline pipe and (b) branched penstock.

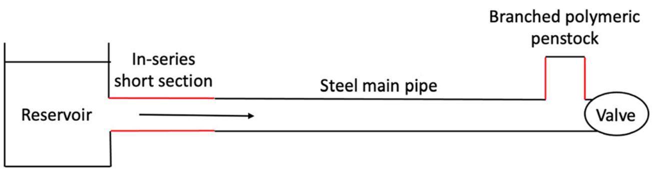

FIG. 31. Dual technique with combined in-series and branched penstock method.

Another surge control method was developed, called the compound technique.[185] This method replaced a single pipe section with two subsections with different materials (HDPE-LDPE). HDPE was attached to the hydraulic part, while LDPE was attached to the steel pipe. This method was found to have a better trade-off between pressure attenuation and wave oscillation than the conventional method. The compound technique for viscoelastic-based surge control is shown in Fig. 32.

Chaker and Triki also adopted the compound method by using two-branched polymeric penstocks with combined LDPE-HDPE pipes,[186] see Fig. 33. This method was observed to have a better trade-off between pressure head attenuation and oscillation wave spreading compared to conventional branched polymeric penstock with the optimum trade-off depending on penstock's diameter and length.

With the compound method and dual method being the two promising tools for surge control based on viscoelasticity, a comparative study between the two methods was performed.[187] Both methods were found to enhance conventional in-line and branching techniques. However, compared with the dual method, the compound method

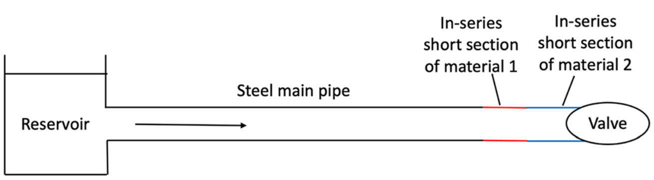

FIG. 32. Compound technique with the in-line pipe.

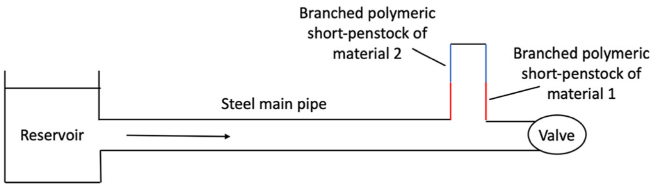

FIG. 33. Compound technique with branched LDPE-HDPE penstock.

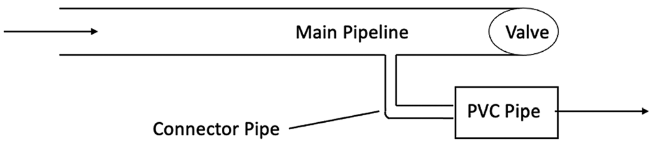

FIG. 34. A proposition to use a viscoelastic branch for surge control.

produced less pressure wave oscillation and emerged as a better surge control method.

While substituting a segment of steel pipe with different configurations of viscoelastic pipes is effective for controlling the transient's peak pressure, the concern is raised regarding its applicability in an existing pipeline system. To solve this issue, Kubrak *et al.*[188] proposed connecting the main pipeline with an additional branch of viscoelastic pipes through a smaller diameter pipe, as shown in Fig. 34. Adopting this method could successfully minimize the peak pressure during transients and shorten the transient period. When analyzed with a varying valve closure time, a longer valve closure time decreased the effectiveness of this method, making it better protection during the rapid transient phenomenon. However, a similar drawback, as observed by Triki,[181] was found in this approach. The use of a smaller diameter connector pipe was also observed to diminish the peak pressure attenuation effectivity of the viscoelastic pipe. In the future, studies may be conducted on the influence of different sizes or material types of connector pipe on the performance of this method.

X. CONCLUSION

This paper is the first literature review on water hammer in viscoelastic pipes. This review aims to provide a summary of the developments in the field of water hammer in viscoelastic pipes, starting from the mathematical model, experimental studies, numerical solutions in the time-domain and the frequency domain, and calibration of viscoelastic parameters, defect detection, and viscoelasticity-based surge control. In the preparation of the manuscript, special attention is dedicated to properly categorizing the relevant progress, e.g., in terms of mathematical modeling or numerical implementation, so that potentials for future works are more elucidated. From this survey, the key research directions are outlined as follows:

- Numerical and mathematical modeling dominates the studies on water hammer in viscoelastic pipes. Regardless of the robust research on numerical implementation, there is currently very limited study on the effect of viscoelasticity in a 3D water hammer model. In the future, more studies on the radial and azimuthal waves and their interactions with longitudinal waves during water hammer in VE pipes are needed.

- A more accurate 1D model shall be proposed to provide better accuracy with less modeling complexity. This accurate 1D model shall incorporate a better material model, UF model, FSI, interaction with the surrounding soil, and cavitating behavior.
- The frequency-domain and time-domain analysis methods are two different approaches for analyzing water hammer problems, each with their advantage and disadvantage. Frequency-domain analysis tools, which include IRM and TMM, are relatively simpler to compute but have a higher error risk due to the linearization procedure. Time-domain analysis tools are accurate in incorporating nonlinear effects but require higher computational requirements. There is a lack of a universal combined method that takes advantage of both while overcoming their drawbacks.
- Calibration of viscoelastic pipes is commonly performed with Kelvin–Voigt elements of up to five elements with increasing accuracy for a higher number of KV elements, coupled with the different optimization algorithms. However, in recent years, researchers have proposed several new viscoelastic parameter calibration schemes, such as step-wise calibration, implemented in the frequency domain and time domain. The correlation between effective viscoelastic parameters to be investigated through experimental and numerical models constitutes a research gap.
- The use of the wave characteristic method for VE pipes has been less appreciated. There is potential in this method to help learn more about the physics of wave propagation in VE pipes.
- In blockage detection, several methods have been proposed, including FRA, coupled PSA-FRA method, and SLE-based method. In the authors' opinion, the PSA-FRA coupled method is a very promising tool for blockage detection. Likewise, the research on leak detection with time-domain tools of ITA, decay law-based detection method, and TDM and recently devised frequency-domain detection tools, including FRF, MFP, and coupled FRF-MFP-MLE method, is quite mature. However, a future improvement in the leak and blockage detection methods for the accurate inclusion/calibration of the viscoelasticity effect seems necessary.
- The use of viscoelastic pipes is a viable surge control measure. While different techniques have been recently proposed, the compound technique is currently the best surge control method. In the future, the compound method may be experimentally validated and modified by a series of short polymeric pipes and branched polymeric penstock of different materials.

ACKNOWLEDGMENTS

This work has been supported by the Research Grants Council of Hong Kong under Project No. 15200719.

AUTHOR DECLARATIONS

Conflict of Interest

The authors have no conflicts to disclose.

Author Contributions

Vincent Tjuatja: Data curation (equal); Formal analysis (equal); Software (equal); Validation (equal); Visualization (equal); Writing – original draft (equal). **Alireza Keramat:** Conceptualization (equal); Data curation (equal); Formal analysis (equal); Methodology (equal); Supervision (equal); Visualization (equal); Writing – original draft (equal); Writing – review & editing (equal). **Bin Pan:** Formal analysis (equal); Investigation (equal); Software (equal); Writing – original draft (equal); Writing – review & editing (equal). **Huan-Feng Duan:** Conceptualization (equal); Funding acquisition (equal); Resources (equal); Writing – review & editing (equal). **Bruno Brunone:** Conceptualization (equal); Resources (equal); Writing – review & editing (equal). **Silvia Meniconi:** Conceptualization (equal); Resources (equal); Writing – review & editing (equal).

DATA AVAILABILITY

The data that support the findings of this study are available from the corresponding author upon reasonable request.

NOMENCLATURE

A	Cross-sectional area
A_j	Cross-section area of j-th cylinder
a_0	Wave speed
BTA	Backward transient analysis
CFD	Computational fluid dynamics
D	Pipe diameter
D/Dt	Material derivative in cylindrical coordinate
DACM	Discrete Adamkowski cavitating model
DGCM	Discrete gas cavity model
DTS	Delayed time scale
DVCM	Discrete vapor cavity model
dV/dt	Local acceleration
E^r	Dynamic modulus of elasticity
e	Pipe wall thickness
FDTBM	Frequency domain transient based method
F_j	Local shear force per unit length of cylinder j
FRA	Frequency response analysis
FRD	Frequency response diagram
FRF	Frequency response function
FRFM	Frequency response function method
FRF-MFP	Frequency response function coupled with matched field processing
FRF-MFP-MLE	Frequency response function coupled with matched field processing and maximum likelihood estimator
FSI	Fluid–structure interaction
f	Body force along the direction of interest
$f_{quas\text{-}steady}$	Quasi-steady friction factor
f_s	Steady friction factor
f_u	Unsteady friction factor
G	Relaxation function
GIVCM	Generalized interface vaporous cavitating model
G_k	Relaxation coefficients
g	Gravitational acceleration
H	Piezometric head
HDPE	High-density polyethylene
HFW	High-frequency waves
IFT	Inverse Fourier transform
IRM	Impulse response method

ITA	Inverse transient analysis
J	Creep compliance
J_0	Creep compliance for the first spring
J_k	Creep compliance of the k-th KV elements
KV	Kelvin-–Voight
k	Brunone's friction coefficient
k_0	Creep parameter
LDPE	Low-density polyethylene
MDPE	Medium-density polyethylene
MFP	Matched field processing
MLE	Maximum likelihood estimator
MOC	Method of characteristics
m_i	Coefficient m in Zielke's weighting function
$\dot{m}_j$	Mass flux of cylinder j
n_i	Coefficient n in Zielke's weighting function
PDE	Partial differential equations
PE	Polyethylene
PolyU	The Hong Kong Polytechnic University
PSA	Pressure signal analysis
PSA-FRA	Pressure signal analysis coupled with frequency response analysis
PVC	Polyvinyl chloride
p	Pressure
Q	Volumetric flow rate
R	Pipe radius
R_0	Initial Reynolds Number
Re	Reynolds number
R_{ve}	Equivalent resistance in the viscoelastic system
r	Radius from the axis
SCE-UA	Shuffled complex evolution of University of Arizona
SLE	Successive linear estimator
SPM	Smoothed particle method
s	Integral dummy variable
TDM	Transient damping method
TMM	Transfer matrix method
t	Time
UF	Unsteady friction
u	Velocity along axial direction
u_j	Velocity along axial direction of cylinder j
V	Average velocity
VE	Viscoelastic
ν	Kinematic viscosity
v	Velocity along radial direction
w	Velocity along azimuthal direction
x	Distance along axial direction
y	Distance along radial direction
1D	One dimension
2D	Two dimension
3D	Three dimension

Greek

α	Pipe wall coefficient
α_{anch}	Coefficient relating to anchors' action
α_r	Averaging factor
$\partial V/\partial x$	Convective acceleration
∇^2	Laplace operator in the cylindrical coordinate
ε^k	Retarded strain of KV element k
ε_r	Retarded strain
η_k	Viscosity of k-th dashpot
θ	Distance along azimuthal direction
κ	Bulk modulus
κ_p	Bulk modulus of pipe material
μ	Dynamic modulus
μ'	Volume viscosity coefficient due to viscoelasticity
ν	Poisson's ratio
ρ	Density
σ	Viscosity ratio
τ	Shear stress; non-dimensional time for Eqs. (28)–(31)
τ_k	Ratio between dashpot's viscosity and spring's elastic modulus
$\hat{\tau}_k$	Relaxation time
τ_r	Retarded time of the dashpots
ψ	Dimensional parameter based on the pipe section dimension and constraint

REFERENCES

[1] M. S. Ghidaoui, "On the fundamental equations of water hammer," Urban Water J. **1**(2), 71–83 (2004).

[2] M. S. Ghidaoui, M. Zhao, D. A. McInnis, and D. H. Axworthy, "A review of water hammer theory and practice," Appl. Mech. Rev. **58**(1–6), 49–75 (2005).

[3] A. Keramat and A. Tijsseling, "Waterhammer with column separation, fluid–structure interaction and unsteady friction in a viscoelastic pipe," CASA-Report No. 1243 (2012).

[4] A. Keramat, A. S. Tijsseling, Q. Hou, and A. Ahmadi, "Fluid–structure interaction with pipe-wall viscoelasticity during water hammer," J. Fluids Struct. **28**, 434–455 (2012).

[5] N. Joukowsky, "On the hydraulic hammer in water supply pipes," Mem. Acad. Imp. Sci. St.-Petersbourg **9**(5), 1–71 (1898).

[6] M. H. Chaudry, *Applied Hydraulic Transients* (Springer, New York, 1987).

[7] R. Skalak, "An extension of the theory of water hammer," Trans. Am. Soc. Mech. Eng. **78**(1), 105–115 (1956).

[8] S. M. Kokoshvili, "Water hammer in a viscoelastic pipe," Polym. Mech. **6**(5), 786–788 (1973).

[9] D. Covas, I. Stoianov, J. F. Mano, H. Ramos, N. Graham, and C. Maksimovic, "The dynamic effect of pipe-wall viscoelasticity in hydraulic transients. II. Model development, calibration and verification," J. Hydraul. Res. **43**(1), 56–70 (2005).

[10] G. Pezzinga and P. Scandura, "Unsteady flow in installations with polymeric additional pipe," J. Hydraul. Eng. **121**(11), 802–811 (1995).

[11] G. Pezzinga, B. Brunone, and S. Meniconi, "Relevance of pipe period on Kelvin–Voigt viscoelastic parameters: 1D and 2D inverse transient analysis," J. Hydraul. Eng. **142**(12), 04016063 (2016).

[12] B. Brunone, B. W. Karney, M. Mecarelli, and M. Ferrante, "Velocity profiles and unsteady pipe friction in transient flow," J. Water Resour. Plann. Manage. **126**(4), 236–244 (2000).

[13] C. Landry, C. Nicolet, A. Bergant, A. Müller, and F Avellan, "Modeling of unsteady friction and viscoelastic damping in piping systems," IOP Conf. Ser.: Earth Environ. Sci. **15**, 2030 (2012).

[14] S. Meniconi, B. Brunone, M. Ferrante, and C. Massari, "Transient hydrodynamics of in-line valves in viscoelastic pressurized pipes: Long-period analysis," Exp. Fluids **53**(1), 265–275 (2012).

[15] G. Pezzinga, B. Brunone, D. Cannizzaro, M. Ferrante, S. Meniconi, and A. Berni, "Two-dimensional features of viscoelastic models of pipe transients," J. Hydraul. Eng. **140**(8), 04014036 (2014).

[16] H. F. Duan, P. J. Lee, M. S. Ghidaoui, and Y.-K. Tung, "System response function–based leak detection in viscoelastic pipelines," J. Hydraul. Eng. **138**(2), 143–153 (2012).

[17]A. Keramat and A. Haghighi, "Straightforward transient-based approach for the creep function determination in viscoelastic pipes," J. Hydraul. Eng. **140**(12), 04014058 (2014).
[18]M. Ferrante and C. Capponi, "Viscoelastic models for the simulation of transients in polymeric pipes," J. Hydraul. Res. **55**(5), 599–612 (2017).
[19]A. Keramat, A. G. Kolahi, and A. Ahmadi, "Waterhammer modelling of viscoelastic pipes with a time-dependent Poisson's ratio," J. Fluids Struct. **43**, 164–178 (2013).
[20]B. Brunone and A. Berni, "Wall shear stress in transient turbulent pipe flow by local velocity measurement," J. Hydraul. Eng. **136**(10), 716–726 (2010).
[21]E. M. Wahba, "On the two-dimensional characteristics of laminar fluid transients in viscoelastic pipes," J. Fluids Struct. **68**, 113–124 (2017).
[22]G. Pezzinga, "Quasi-2D model for unsteady flow in pipe networks," J. Hydraul. Eng. **125**(7), 676–685 (1999).
[23]H. F. Duan, M. Ghidaoui, P. J. Lee, and Y. K. Tung, "Unsteady friction and visco-elasticity in pipe fluid transients," J. Hydraul. Res. **48**(3), 354–362 (2010).
[24]H. Shamloo and M. Mousavifard, "Numerical simulation of turbulent pipe flow for water hammer," J. Fluids Eng., Trans. ASME **137**(11), 111203 (2015).
[25]M. Louati and M. S. Ghidaoui, "High-frequency acoustic wave properties in a water-filled pipe. II. Range of propagation," J. Hydraul. Eng. **55**(5), 632–646 (2017).
[26]M. Louati and M. S. Ghidaoui, "High-frequency acoustic wave properties in a water-filled pipe. I. Dispersion and multi-path behaviour," J. Hydraul. Res. **55**(5), 613–631 (2017).
[27]Z. Lai, M. Louati, S. Nasraoui, and M. Ghidaoui, "Numerical investigation of high frequency wave-leak interaction in water-filled pipes," J. Hydraul. Eng. **147**(1), 04020091 (2021).
[28]S. Saemi, M. Raisee, M. J. Cervantes, and A. Nourbakhsh, "Computation of two- and three-dimensional water hammer flows," J. Hydraul. Res. **57**(3), 386–404 (2019).
[29]M. A. Siba, W. M. F. Mahmood, M. Z. Nuawi, R. Rasani, and M. H. Nassir, "Modeling and applications of 3D flow in orifice plate at low turbulent Reynold numbers," Int. J. Mech. Mechatron. Eng. **15**(4), 19–25 (2015).
[30]M. S. Shah, J. B. Joshi, A. S. Kalsi, C. S. R. Prasad, and D. S. Shukla, "Analysis of flow through an orifice meter: CFD simulation," Chem. Eng. Sci. **71**, 300–309 (2012).
[31]M. Shehadeh, A. Sharara, M. Khamis, and H. El-Gamal, "A study of pipeline leakage pattern using CFD," Can. J. Mech. Sci. Eng. **3**(3), 98–101 (2012).
[32]M. Morvarid, A. Rezghi, A. Riasi, and M. Haghighi Yazdi, "3D numerical simulation of laminar water hammer considering pipe wall viscoelasticity and the arbitrary Lagrangian–Eulerian method," World J. Eng. **15**(2), 298–305 (2018).
[33]R. B. Carmona-Paredes, R. Autrique, E. Rodal-Canales, and D. Paniagua-Lovera, "A new method to calculate hydraulic transients in HDPE pipes using the standard solid model to represent the HDPE viscoelastic behaviour," IOP Conf. Ser.: Earth Environ. Sci. **240**, 052020 (2019).
[34]M. Hino, M. Sawamoto, and S. Takasu, "Study on the transition to turbulence and frictional coefficient in an oscillatory pipe flow," Trans. JSCE **9**, 282–284 (1977).
[35]H. Brekke, *A Stability Study on Hydro Power Plant Governing Including the Influence From a Quasi Nonlinear Damping of Oscillatory Flow and From The Turbine Characteristics* (Kvaerner Brug, 1984), Vol. 1.
[36]J. W. Daily, W. L. Hankey, Jr., R. W. Olive, and J. M. Jordaan, Jr., "Resistance coefficients for accelerated and decelerated flows through smooth tubes and orifices," Trans. Am. Soc. Mech. Eng. **78**(5), 1071–1077 (1956).
[37]M. R. Carstens and J. E. Roller, "Boundary-shear stress in unsteady turbulent pipe flow," J. Hydraul. Div. **85**(2), 67–81 (1959).
[38]E. B. Shuy, "Wall shear stress in accelerating and decelerating turbulent pipe flows," J. Hydraul. Res. **34**(2), 173–183 (1996).
[39]B. Brunone, U. M. Golia, and M. Greco, "Some remarks on the momentum equation for fast transients," in *Proceedings of the International Meeting on Hydraulic Transients with Column Separation* (Universidad Politecnica de Valencia, 1991), pp. 201–209.
[40]B. Brunone, U. M. Golia, and M. Greco, "The effects of two dimensionality on pipe transients modeling," J. Hydraul. Eng. **121**(12), 906–912 (1995).
[41]B. Brunone and U. M. Golia, "Discussion of 'Systematic evaluation of one-dimensional unsteady friction models in simple pipelines' by J. P. Vitkovsky, A. Bergant, A. R. Simpson, and M. F. Lamber," J. Hydraul. Eng. **134**(2), 282–284 (2008).
[42]A. Bergant, A. R. Simpson, and J. Vítkovský, "Developments in unsteady pipe flow friction modelling," J. Hydraul. Res. **39**(3), 249–257 (2001).
[43]A. E. Vardy and K. L. Hwang, "A characteristics model of transient friction in pipes," J. Hydraul. Res. **29**(5), 669–684 (1991).
[44]D. J. Wood and J. E. Funk, "A boundary-layer theory for transient viscous losses in turbulent flow," J. Basic Eng. **92**(4), 865–873 (1970).
[45]O Bratland, "Frequency-dependent friction and radial kinetic energy variation in transient pipe flow," in *5th International Conference on Pressure Surges* (BHRA, 1986), pp. 95–101.
[46]R Vennatrø, "Unsteady friction in pipeline," in 18th IAHR Symposium (Valencia) (1996).
[47]B. Svingen, "Rayleigh damping as an approximate model for transient hydraulic pipe friction," in 8th International Meeting of the IAHR Work Group on the Behaviour of Hydraulic Machinery under Steady Oscillatory Conditions (1997).
[48]W. Zielke, "Frequency-dependent friction in transient pipe flow," J. Basic Eng. **90**(1), 109–115 (1968).
[49]A. E. Vardy and K.-L. Hwang, "A weighting function model of transient turbulent pipe friction," J. Hydraul. Res. **31**(4), 533–548 (1993).
[50]A. E. Vardy and J. M. Brown, "Transient, turbulent, smooth pipe friction," J. Hydraul. Res. **33**(4), 435–456 (1995).
[51]A. E. Vardy and J. M. B. Brown, "Transient turbulent friction in smooth pipe flows," J. Sound Vib. **259**(5), 1011–1036 (2003).
[52]K. Urbanowicz, Z. Zarzycki, and S. Kudźma, "Universal weighting function in modeling transient cavitating pipe flow," J. Theor. Appl. Mech. **50**(4), 889–902 (2012).
[53]A. K. Trikha, "An efficient method for simulating frequency-dependent friction in transient liquid flow," J. Fluids Eng. **97**(1), 97–105 (1975).
[54]T. Kagawa, I. Lee, A. Kitagawa, and T. Takenaka, "High speed and accurate computing method of frequency-dependent friction in laminar pipe flow for characteristics method," SME Int. J., Ser. B **49**(447), 2638–2644 (1983).
[55]A. Vardy and J. Brown, "Efficient approximation of unsteady friction weighting functions," J. Hydraul. Eng. **130**(11), 1097–1107 (2004).
[56]J. P. Vítkovský, M. L. Stephens, A. Bergant, and M. F. Lambert, "Efficient and accurate calculation of Zielke and Vardy-Brown unsteady friction in pipe transients," in *Proceedings of the 9th International Conference on Pressure Surges* (BHR Group, 2004), pp. 405–419.
[57]Z. Zarzycki, S. Kudźma, and K. Urbanowicz, "Improved method for simulating transients of turbulent pipe flow," J. Theor. Appl. Mech. **49**(1), 135–158 (2011).
[58]K. Urbanowicz, "Analytical expressions for effective weighting functions used during simulations of water hammer," J. Theor. Appl. Mech. **55**(3), 1029–1040 (2017).
[59]B. W. Karney, "Energy relations in transient closed-conduit flow," J. Hydraul. Eng. **116**(10), 1180–1196 (1990).
[60]H. F. Duan, M. S. Ghidaoui, and Y. K. Tung, "Energy analysis of viscoelasticity effect in pipe fluid transients," J. Appl. Mech., Trans. ASME **77**(4), 044503 (2010).
[61]K. Wu, Y. Feng, Y. Xu, H. Liang, and G. Liu, "Energy analysis of a quasi-two-dimensional friction model for simulation of transient flows in viscoelastic pipes," Water **14**(20), 3258 (2022).
[62]P. J. Lee, "Energy analysis for the illustration of inaccuracies in the linear modelling of pipe fluid transients," J. Hydraul. Res. **51**(2), 133–144 (2013).
[63]B. Pan, A. Keramat, C. Capponi, S. Meniconi, B. Brunone, and H. Duan, "Transient energy analysis in water-filled viscoelastic pipelines," J. Hydraul. Eng. **148**(1), 04021051 (2022).
[64]G. Thibessard, "The simulation of water hammer on a numerical calculator," in *9th IAHR Convention, Dubrovnik, Yugoslavia* (IAHR, 1961), pp. 881–890.
[65]V. L. Streeter, "Water hammer analysis," J. Hydraul. Div. **95**(6), 1959–1972 (1969).
[66]T. Tanahashi and E. Kasahara, "Analysis of the waterhammer with water column separation," Bull. JSME **12**(50), 206–214 (1969).
[67]E. B. Wylie and V. L. Streeter, "Column separation in horizontal pipelines," in *Proceedings of the Joint Symposium on Design and Operation of Fluid Machinery* (IAHR/ASME/ASCE, 1978), pp. 3–13.

[68]E. B Wylie, V. L Streeter, and L Suo, *Fluid Transients in Systems* (Prentice Hall, 1993).
[69]A. Bergant, A. Simpson, and A. Tijsseling, "Water hammer with column separation: A historical review," J. Fluids Struct. **22**(2), 135–171 (2006).
[70]A. Bergant, A. S. Tijsseling, J. P. Vítkovský, D. I. C. Covas, A. R. Simpson, and M. F. Lambert, "Parameters affecting water-hammer wave attenuation, shape and timing. I. Mathematical tools," J. Hydraul. Res. **46**(3), 373–381 (2008).
[71]A. Keramat, A. S. Tijsseling, and A. Ahmadi, "Investigation of transient cavitating flow in viscoelastic pipes," IOP Conf. Ser.: Earth Environ. Sci. **12**, 012081 (2010).
[72]A. K. Soares, D. I. C. Covas, and N. J. G. Carrio, "Transient vaporous cavitation in viscoelastic pipes," J. Hydraul. Res. **50**(2), 228–235 (2012).
[73]A. K Soares, N Martins, and D. I. C Covas, "Investigation of transient vaporous cavitation: Experimental and numerical analyses," Procedia Eng. **119**, 235–242 (2015).
[74]L. Hadj-Taïeb and E. Hadj-Taïeb, "Numerical simulation of transient flows in viscoelastic pipes with vapour cavitation," Int. J. Modell. Simul. **29**(2), 206–213 (2009).
[75]A. Bergant and A. R. Simpson, "Pipeline column separation flow regimes," J. Hydraul. Eng. **125**(8), 835–848 (1999).
[76]A. R Simpson, *Large Water Hammer Pressures Due to Column Separation in Sloping Pipes (Transients, Cavitation)* (University of Michigan, 1986).
[77]R. J. Brown, "Water-column separation at two pumping plants," J. Basic Eng. **90**(4), 521–530 (1968).
[78]A. H. De Vries, *Cavitation Due to Waterhammer in Horizontal Pipelines with Several High Points* (Delft Hydraulics Laboratory , 1973).
[79]G. A. Provoost, *Investigation into Cavitation in a Prototype Pipeline Caused by Water Hammer* (BHRA, 1976).
[80]G. A. Provoost and E. B. Wylie, "Discrete gas model to represent distributed free gas in liquids," in *5th International Symposium on Water Column Separation* (IAHR, 1982), pp. 28–30.
[81]E. B. Wylie, "Simulation of vaporous and gaseous cavitation," J. Fluids Eng. **106**, 307–311 (1984).
[82]C. Kranenburg, *Transient Cavitation in Pipelines* (Delft University of Technology, 1974).
[83]K. Urbanowicz and M. Firkowski, "Extended bubble cavitation model to predict water hammer in viscoelastic pipelines," J. Phys.: Conf. Ser. **1101**, 012046 (2018).
[84]K. Urbanowicz, A. Bergant, and H. F. Duan, "Simulation of unsteady flow with cavitation in plastic pipes using the discrete bubble cavity and Adamkowski model," IOP Conf. Ser.: Mater. Sci. Eng. **710**, 012013 (2019).
[85]A. Bergant and A. R. Simpson, "Interface model for transient cavitating flow in pipelines," in *Unsteady Flow and Fluid Transients*, edited by R. Bettess and J. Watts (A. A. Balkema, 1992), pp. 333–342.
[86]M. Sadafi, A. Riasi, and S. A. Nourbakhsh, "Cavitating flow during water hammer using a generalized interface vaporous cavitation model," J. Fluids Struct. **34**, 190–201 (2012).
[87]A. S. Tijsseling, M. F. Lambert, A. R. Simpson, M. L. Stephens, J. P. Vítkovský, and A. Bergant, "Skalak's extended theory of water hammer," J. Sound Vib. **310**(3), 718–728 (2008).
[88]A. S. Tijsseling, "Fluid–structure interaction in liquid-filled pipe systems: A review," J. Fluids Struct. **10**(2), 109–146 (1996).
[89]Z. M. Wang and S. K. Eat Tan, "Coupled analysis of fluid transients and structural dynamic responses of a pipeline system," J. Hydraul. Res. **35**(1), 119–131 (1997).
[90]L. Zhang, S. A. Tijsseling, and E. A. Vardy, "FSI analysis of liquid-filled pipes," J. Sound Vib. **224**(1), 69–99 (1999).
[91]D. C. Wiggert and A. S. Tijsseling, "Fluid transients and fluid–structure interaction in flexible liquid-filled piping," Appl. Mech. Rev. **54**(5), 455–481 (2001).
[92]D. Ferras, "Fluid–structure-interaction in pipe coils during hydraulic transients: Numerical and experimental analysis," in *E-Proceedings of the 36th IAHR World Congress* (IAHR, 2015), Vol. 28.
[93]D. Ferràs, P. A. Manso, A. J. Schleiss, and D. I. Covas, "Fluid–structure interaction in straight pipelines: Friction coupling mechanisms," Comput. Struct. **175**, 74–90 (2016).
[94]J. S. Walker and J. W. Phillips, "Pulse propagation in fluid-filled tubes," J. Appl. Mech. **44**(1), 31–35 (1977).
[95]R. A. Valentin, J. W. Phillips, and J. S. Walker, *Reflection and Transmission of Fluid Transients at an Elbow* (Argonne National Laboratory, 1979).
[96]D. C. Wiggert, F. J. Hatfield, and S. Stuckenbruck, "Analysis of liquid and structural transients in piping by the method of characteristics," J. Fluids Eng. **109**(2), 161–165 (1987).
[97]S. Henclik, "Numerical modeling of water hammer with fluid–structure interaction in a pipeline with viscoelastic supports," J. Fluids Struct. **76**, 469–487 (2018).
[98]M. A. Guidara, L. Hadj Taieb, C. Schmitt, E. H. Taieb, and Z. Azari, "Investigation of viscoelastic effects on transient flow in a relatively long PE100 pipe," J. Fluids Struct. **80**, 370–389 (2018).
[99]H. K. Aliabadi, A. Ahmadi, and A. Keramat, "Frequency response of water hammer with fluid–structure interaction in a viscoelastic pipe," Mech. Syst. Signal Process. **144**, 106848 (2020).
[100]R. Zanganeh, A. Ahmadi, and A. Keramat, "Fluid–structure interaction with viscoelastic supports during waterhammer in a pipeline," J. Fluids Struct. **54**, 215–234 (2015).
[101]S. Henclik, "A numerical approach to the standard model of water hammer with fluid–structure interaction," J. Theor. Appl. Mech. **53**(3), 543–555 (2015).
[102]R. Sadat Hosseini, A. Ahmadi, and R. Zanganeh, "Fluid–structure interaction during water hammer in a pipeline with different performance mechanisms of viscoelastic supports," J. Sound Vib. **487**, 115527 (2020).
[103]D. Covas, I. Stoianov, J. F. Mano, H. Ramos, N. Graham, and C. Maksimovic, "The dynamic effect of pipe-wall viscoelasticity in hydraulic transients. I. Experimental analysis and creep characterization," J. Hydraul. Res. **42**(5), 517–532 (2004).
[104]H. Ramos and D. Covas, "Water pipe system response under dynamic effects," J. Water Supply: Res. Technol. **55**(4), 269–282 (2006).
[105]X. Wang, J. Lin, A. Keramat, M. S. Ghidaoui, S. Meniconi, and B. Brunone, "Matched-field processing for leak localization in a viscoelastic pipe: An experimental study," Mech. Syst. Signal Process. **124**, 459–478 (2019).
[106]A. Keramat, M. Fathi-Moghadam, R. Zanganeh, M. Rahmanshahi, A. S. Tijsseling, and E Jabbari, "Experimental investigation of transients-induced fluid–structure interaction in a pipeline with multiple-axial supports," J. Fluids Struct. **93**, 102848 (2020).
[107]I. Rezapour, M. S. Bejestan, and B. Aminnejad, "Case study of leak detection based on Gaussian function in experimental viscoelastic water pipeline," Water Supply **21**(7), 3860–3874 (2021).
[108]H. A. Warda, H. A. Kandil, A. A. Elmiligui, and E. M. Wahba, "Modeling pressure transients in viscoelastic pipes," Alexandria Eng. J. **40**(6), 797–809 (2001).
[109]C. Apollonio, D. I. C. Covas, G. de Marinis, A. Leopardi, and H. M. Ramos, "Creep functions for transients in HDPE pipes," Urban Water J. **11**(2), 160–166 (2014).
[110]N. Carriço, A. K. Soares, and D. Covas, *Calibration Methodology for Hydraulic Transient Solvers Incorporating Unsteady Friction and Pipe Wall Viscoelasticity* (Universidade Téchnica de Liboa, 2015).
[111]D. Ferràs, P. A. Manso, A. J. Schleiss, and D. I. C. Covas, "Experimental distinction of damping mechanisms during hydraulic transients in pipe flow," J. Fluids Struct. **66**, 424–446 (2016).
[112]H. A. Warda, I. G. Adam, and A. B. Rashad, "Modeling pressure transient due to valve closure in leaking viscoelastic," Alexandria Eng. J. **46**(5), 621–638 (2007).
[113]C. Apollonio, G. De Marinis, A. Leopardi, and C. Apollonio, "Water hammer in viscoelastic pipes. The effect of junctions-first results," in Proceedings of the XXXIV IAHR Congress (2009).
[114]D. J. Wood and S. P. Chao, "Effect of pipelines junctions on water hammer surges," Transp. Eng. J. **97**(3), 441–457 (1971).
[115]S. Evangelista, A. Leopardi, R. Pignatelli, and G. de Marinis, "Hydraulic transients in viscoelastic branched pipelines," J. Hydraul. Eng. **141**(8), 04015016 (2015).
[116]M. Ferrante and C. Capponi, "Calibration of viscoelastic parameters by means of transients in a branched water pipeline system," Urban Water J. **15**(1), 9–15 (2018).

[117]M. Ferrante, B. Brunone, and S. Meniconi, "Leak detection in branched pipe systems coupling wavelet analysis and a Lagrangian model," J. Water Supply: Res. Technol. **58**(2), 95–106 (2009).

[118]S. Meniconi, F. Maietta, S. Alvisi, C. Capponi, V. Marsili, M. Franchini, and B. Brunone, "A quick survey of the most vulnerable areas of a water distribution network due to transients generated in a service line: A Lagrangian model based on laboratory tests," Water Resour. Res. **14**(17), 2741, https://doi.org/10.3390/w14172741 (2022).

[119]S. Meniconi, F. Maietta, S. Alvisi, C. Capponi, V. Marsili, M. Franchini, and B. Brunone, "Consumption change-induced transients in a water distribution network: Laboratory tests in a looped system," Water Resour. Res. **58**(10), e2021WR031343, https://doi.org/10.1029/2021WR031343 (2022).

[120]S. Meniconi, B. Brunone, and M. Ferrante, "Water-hammer pressure waves interaction at cross-section changes in series in viscoelastic pipes," J. Fluids Struct. **33**, 44–58 (2012).

[121]C. Massari, T. C. J. Yeh, M. Ferrante, B. Brunone, and S. Meniconi, "A stochastic tool for determining the presence of partial blockages in viscoelastic pipelines: First experimental results," Procedia Eng. **70**, 1112–1120 (2014).

[122]M. Fathi-Moghadam and S. Kiani, "Simulation of transient flow in viscoelastic pipe networks," J. Hydraul. Res. **58**(3), 531–540 (2020).

[123]D. Covas, I. Stoianov, H. Ramos, N. Graham, Č. Maksimović, and D. Butler, "Water hammer in pressurized polyethylene pipes: Conceptual model and experimental analysis," Urban Water J. **1**(2), 177–197 (2004).

[124]A. Bergant, Q. Hou, A. Keramat, and A. S. Tijsseling, "Experimental and numerical analysis of water hammer in a large-scale PVC pipeline apparatus," in 4th International Meeting on Cavitation and Dynamic Problems in Hydraulic Machinery and Systems (2011).

[125]A. Bergant, Q. Hou, A. Keramat, and A. S. Tijsseling, "Waterhammer tests in a long PVC pipeline with short steel end sections," J. Hydraul. Struct. **1**(1), 24–36 (2013).

[126]M. L. Stephens, M. F. Lambert, A. R. Simpson, and J. P. Vitkovsky, "Calibrating the water-hammer response of a field pipe network by using a mechanical damping model," J. Hydraul. Eng. **137**(10), 1225–1237 (2011).

[127]K. Weinerowska-Bords, "Alternative approach to convolution term of viscoelasticity in equations of unsteady pipe flow," J. Fluids Eng., Trans. ASME **137**(5), 054501 (2015).

[128]P.-G. Franke, "Computation of unsteady pipe flow with respect to visco-elastic material properties," J. Hydraul. Res. **21**(5), 345–353 (1983).

[129]M. B. Abbott, *An Introduction to the Method of Characteristics* (American Elsevier, 1966).

[130]K. Urbanowicz and M. Firkowski, "Effect of creep compliance derivative in modeling water hammer in viscoelastic pipes," in *Pressure Surges* (BHR Group, 2018), Vol. 13, pp. 305–324.

[131]G. Bertaglia, M. Ioriatti, A. Valiani, M. Dumbser, and V. Caleffi, "Numerical methods for hydraulic transients in visco-elastic pipes," J. Fluids Struct. **81**, 230–254 (2018).

[132]J. Rahimi Firuz, S. R. Sabagh Yazdi, and A. Keramat, "Numerical methods of visco-elastic segments on water hammer pressures," Int. J. Numer. Methods Civil Eng. **4**(4), 49–57 (2020).

[133]A. Lazhar, L. Hadj-Taïeb, and E. Hadj-Taïeb, "Two leaks detection in viscoelastic pipeline systems by means of transient," J Loss Prev. Process Ind. **26**(6), 1341–1351 (2013).

[134]A. T. Nile, B. Djebedjian, and M. A. El-Naggar, "Numerical and experimental study of water hammer in viscoelastic pipes with and without extended partial blockage," Mansoura Eng. J. **43**(3), 1–13 (2020).

[135]D. J. Wood, R. G. Dorsch, and C. Lightner, "Wave-plan analysis of unsteady flow in closed conduits," J. Hydraul. Div. **92**(2), 83–110 (1966).

[136]H. A. A. Abdel-Gawad and B. Djebedjian, "Modeling water hammer in viscoelastic pipes using the wave characteristic method," Appl. Math. Model. **83**, 322–341 (2020).

[137]A. Seck, "Numerical solutions of hyperbolic systems of conservation laws combining unsteady friction and viscoelastic pipes," J. Hydroinf. **23**(1), 103–116 (2021).

[138]A. Seck, M. Fuamba, and R. Kahawita, "Finite-volume solutions to the water-hammer equations in conservation form incorporating dynamic friction using the Godunov scheme," J. Hydraul. Eng. **143**(9), 04017029 (2017).

[139]W. Ning, Z. Ling, L. Yunjie, and P. Tianwen, "Finite volume model of water column separation and rejoining water hammer in viscoelastic pipes," Chin. J. Theor. Appl. Mech. **54**(7), 1952–1960 (2022).

[140]P. J. Lee, H. F. Duan, M. Ghidaoui, and B. Karney, "Frequency domain analysis of pipe fluid transient behaviour," J. Hydraul. Res. **51**(6), 609–622 (2013).

[141]D. I. C. Covas, H. M. Ramos, and A. B. De Almeida, "Impulse response method for solving hydraulic transients in viscoelastic pipes," in XXXI IAHR Congress (2005).

[142]C. Capponi, A. C. Zecchin, M. Ferrante, and J. Gong, "Numerical study on accuracy of frequency-domain modelling of transients," J. Hydraul. Res. **55**(6), 813–828 (2017).

[143]P. J. Lee, M. F. Lambert, A. R. Simpson, J. P. Vítkovský, and J. Liggett, "Experimental verification of the frequency response method for pipeline leak detection," J. Hydraul. Res. **44**(5), 693–707 (2006).

[144]A. Keramat, B. Karney, M. S. Ghidaoui, and X. Wang, "Transient-based leak detection in the frequency domain considering fluid–structure interaction and viscoelasticity," Mech. Syst. Signal Process. **153**, 107500 (2021).

[145]B. Pan, H. F. Duan, S. Meniconi, and B. Brunone, "FRF-based transient wave analysis for the viscoelastic parameters identification and leak detection in water-filled plastic pipes," Mech. Syst. Signal Process. **146**, 107056 (2021).

[146]H. F. Duan, P. J. Lee, M. S. Ghidaoui, and Y. K. Tung, "Extended blockage detection in pipelines by using the system frequency response analysis," J. Water Resour. Plann. Manage. **138**(1), 55–62 (2012).

[147]B. Pan, H. F. Duan, S. Meniconi, K. Urbanowicz, T. C. Che, and B. Brunone, "Multistage frequency-domain transient-based method for the analysis of viscoelastic parameters of plastic pipes," J. Hydraul. Eng. **146**(3), 04019068 (2020).

[148]K. Weinerowska-Bords, "Viscoelastic model of waterhammer in single pipeline-problems and questions," Arch. Hydro-Eng. Environ. Mech. **53**(4), 331–351 (2006).

[149]D. Covas and H. Ramos, "Case studies of leak detection and location in water pipe systems by inverse transient analysis," J. Water Resour. Plann. Manage. **136**(2), 248–257 (2010).

[150]A. K. Soares, D. I. Covas, L. Fernanda, and R. Reis, "Analysis of PVC pipe-wall viscoelasticity during water hammer," J. Hydraul. Eng. **134**(9), 1389 (2008).

[151]G. Pezzinga, "Evaluation of time evolution of mechanical parameters of polymeric pipes by unsteady flow runs," J. Hydraul. Eng. **140**(12), 04014057 (2014).

[152]M. Ferrante and C. Capponi, "Comparison of viscoelastic models with a different number of parameters for transient simulations," J. Hydroinf. **20**(1), 1–17 (2018).

[153]J. J. O. Cheshme, A. Ahmadi, A. Keramat, and A. S. Arniazi, "Sensitivity of creep coefficients to the fundamental water hammer period in viscoelastic pipes," Urban Water J. **18**(3), 183–194 (2021).

[154]M. J. Potvin, "Comparison of time-domain finite element modelling of viscoelastic structures using an efficient fractional Voigt–Kelvin model or Prony series," Ph.D. thesis (McGill University, 2001).

[155]J. Gong, A. C. Zecchin, M. F. Lambert, and A. R. Simpson, "Determination of the creep function of viscoelastic pipelines using system resonant frequencies with hydraulic transient analysis," J. Hydraul. Eng. **142**(9), 04016023 (2016).

[156]H. F. Duan, B. Pan, M. Wang, L. Chen, F. Zheng, and Y Zhang, "State-of-the-art review on the transient flow modelling and utilization for urban water supply system (UWSS) management," J. Water Supply: Res. Technol. **69**(8), 858–893 (2020).

[157]B. Brunone, F. Maietta, C. Capponi, H. F. Duan, and S. Meniconi, "Detection of partial blockages in pressurized pipes by transient tests. A review of the physical experiments," Fluids **8**(1), 19 (2023).

[158]S. Meniconi, H. F. Duan, P. J. Lee, B. Brunone, M. S. Ghidaoui, and M. Ferrante, "Experimental investigation of coupled frequency and time-domain transient test–based techniques for partial blockage detection in pipelines," J. Hydraul. Eng. **139**(10), 1033–1040 (2013).

[159]S. Meniconi, B. Brunone, and M. Ferrante, "In-line pipe device checking by short-period analysis of transient tests," J. Hydraul. Eng. **137**(7), 713–722 (2011).

[160]C. Massari, T. C. J. Yeh, M. Ferrante, B. Brunone, and S. Meniconi, "A stochastic approach for extended partial blockage detection in viscoelastic pipelines: Numerical and laboratory experiments," J. Water Supply: Res. Technol. **64**(5), 583–595 (2015).

[161]P. Kumar and P. K. Mohapatra, "Partial blockage detection in pipelines by modified reconstructive method of characteristics technique," J. Hydraul. Eng. **148**(4), 04022003 (2022).
[162]B. Brunone, F. Maietta, C. Capponi, A. Keramat, and S. Meniconi, "A review of physical experiments for leak detection in water pipes through transient tests for addressing future research," J. Hydraul. Res. **60**(6), 894–906 (2022).
[163]R. S. Pudar and J. A. Liggett, "Leaks in pipe networks," J. Hydraul. Eng. **118**(7), 1031–1046 (1992).
[164]J. A. Liggett and L. C. Chen, "Inverse transient analysis in pipe networks," J. Hydraul. Eng. **120**(8), 934–955 (1994).
[165]K. Tang, B. Karney, M. Pendlebury, and F. Zhang, "Inverse transient calibration of water distribution systems using genetic algorithms," in *Water Industry Systems: Modelling and Optimization Applications* (Research Studies Press, 1999), Vol. 1.
[166]Z. S. Kapelan, D. A. Savic, and G. A. Walters, "A hybrid inverse transient model for leakage detection and roughness calibration in pipe networks," J. Hydraul. Res. **41**(5), 481–492 (2003).
[167]J. Vitkovsky, J. Liggett, A. Simpson, and M. Lambert, "Optimal measurement site locations for inverse transient analysis in pipe networks," J. Water Resour. Plann. Manage. **129**(6), 480–492 (2003).
[168]A. F. Colombo, P. Lee, and B. W. Karney, "A selective literature review of transient-based leak detection methods," J. Hydro-Environ. Res. **2**(4), 212–227 (2009).
[169]A. K. Soares, D. I. Covas, and L. F. R. Reis, "Leak detection by inverse transient analysis in an experimental PVC pipe system," J. Hydroinf. **13**(2), 153–166 (2011).
[170]O. Choura, C. Capponi, S. Meniconi, S. Elaoud, and B. Brunone, "A Nelder–Mead algorithm-based inverse transient analysis for leak detection and sizing in a single pipe," Water Sci. Technol. Water Supply **21**(4), 1580–1593 (2021).
[171]M. Mousavifard, F. Poursmaeili, and H. Shamloo, "Development of backward transient analysis in visco-elastic pressurized pipes," J. Hydraul. Res. **60**(3), 423–433 (2022).
[172]X. Wang, "Fast computation of inverse transient analysis for pipeline condition assessment via surrogate modeling with sparse sampling strategy," Mech. Syst. Signal Process. **162**, 107995 (2022).
[173]X. Wang, M. Lambert, A. Simpson, J. Liggett, and J. Vítkovsky, "Leak detection in pipelines using the damping of fluid transients," J. Hydraul. Eng. **128**(7), 697–711 (2002).
[174]W. Nixon, M. S. Ghidaoui, and A. A. Kolyshkin, "Range of validity of the transient damping leakage detection method," J. Hydraul. Eng. **132**(9), 944–957 (2006).
[175]B. Brunone, S. Meniconi, C. Capponi, and M. Ferrante, "Leak-induced pressure decay during transients in viscoelastic pipes," Procedia Eng. **119**, 243–252 (2015).
[176]B. Brunone, S. Meniconi, and C. Capponi, "Numerical analysis of the transient pressure damping in a single polymeric pipe with a leak," Urban Water J. **15**(8), 760–768 (2018).
[177]C. Capponi, S. Meniconi, P. J. Lee, B. Brunone, and M. Cifrodelli, "Time-domain analysis of laboratory experiments on the transient pressure damping in a leaky polymeric pipe," Water Resour. Manage. **34**(2), 501–514 (2020).
[178]A. Triki, "Water-hammer control in pressurized-pipe flow using an in-line polymeric short-section," Acta Mech **227**(3), 777–793 (2016).
[179]A. S. Tijsseling, A. Kruisbrink, and A. Pereira da Silva, "The reduction of pressure wavespeeds by internal rectangular cubes," in *3rd ASME & JSME Joint Fluids Engineering Conference, Symposium S-290 Water Hammer* (ASME, 1999).
[180]A. Triki, "Water-hammer control in pressurized-pipe flow using a branched polymeric penstock," J. Pipeline Syst. Eng. Pract. **8**(4), 04017024 (2017).
[181]A. Triki, "Further investigation on water-hammer control inline strategy in water-supply systems," J. Water Supply: Res. Technol. **67**(1), 30–43 (2018).
[182]A. Triki, "Dual-technique-based inline design strategy for water-hammer control in pressurized pipe flow," Acta Mech. **229**(5), 2019–2039 (2018).
[183]M. Trabelsi and A. Triki, "Dual control technique for mitigating water-hammer phenomenon in pressurized steel-piping systems," Int. J. Pressure Vessels Piping **172**, 397–413 (2019).
[184]A. Triki and M. Trabelsi, "On the in-series and branching dual-technique-based water-hammer control strategy," Urban Water J. **18**(8), 631–639 (2021).
[185]A. Triki and M. A. Chaker, "Compound technique-based inline design strategy for water-hammer control in steel pressurized-piping systems," Int. J. Pressure Vessels Piping **169**, 188–203 (2019).
[186]M. A. Chaker and A. Triki, "Investigating the branching redesign strategy for surge control in pressurized steel piping systems," Int. J. Pressure Vessels Piping **180**, 104044 (2020).
[187]W. Ben Amira and A. Triki, "Benchmarking the dual and compound techniques-based branching design strategy used for upgrading of pressurized hydraulic systems," J. Pressure Vessel Technol., Trans. ASME **143**(2), 021701 (2021).
[188]M. Kubrak, A. Malesińska, A. Kodura, K. Urbanowicz, P. Bury, and M. Stosiak, "Water hammer control using additional branched HDPE pipe," Energies **14**(23), 8008 (2021).
[189]J. Javadi Orte Cheshme, A. Ahmadi, and A. Keramat, "Modeling of nonlinear viscoelastic creep of a polyethylene pipeline during water hammer," Urban Water J. **19**(4), 336–347 (2022).